新疆青河县科克辉长岩体：氧化地幔楔部分熔融岩浆的记录

张永[1)]，徐兴旺[2)]

1）中国地质调查局天津地质调查中心，天津，300170；

2）中国科学院地质与地球物理研究所，北京，100029

内容提要：新疆阿尔泰地区科克辉长岩位于额尔齐斯断裂和可可托海-二台断裂交汇部位的东南侧，为探矿过程中发现的隐伏岩体。本次工作对科克辉长岩体地质、年代学和地球化学进行了系统研究，结果显示科克辉长岩体锆石SIMS U-Pb同位素年龄为291Ma左右，对应于早二叠世，岩体具有较低SiO_2（46.14%～52.53%）和MgO（3.00%～7.68%）含量，较低La/Sm（2.56～4.10）和较高的$(Gd/Yb)_N$（1.12～1.61）比值，微量元素具富集大离子亲石元素（K，Rb，Pb等）、亏损高场强元素（Nb与Ta等）等地球化学特征，指示科克辉长岩的岩浆起源于氧化的俯冲交代地幔源区的部分熔融，在上升侵位过程中受外来物质混染作用较弱的特点。综合地质和地球化学特征显示，新疆阿尔泰地区二叠纪科克辉长岩形成于伸展构造背景，岩浆侵位受额尔齐斯断裂走滑作用控制，该岩浆岩是北疆地区广泛发育的二叠纪基性岩浆岩的组成部分。

关键词：辉长岩体；成岩年代；岩石成因；科克地区；阿尔泰

阿尔泰造山带地处准噶尔盆地北缘，是中亚造山带（CAOB）的重要组成部分（Sengör et al.，1993；Xiao Wenjiao et al.，2003）。阿尔泰造山带由一系列陆块、岛弧和增生杂岩构成的增生型造山带，由北向南可分为阿尔泰构造带、南阿尔泰构造带、琼乎尔-阿巴宫构造带、额尔齐斯构造带以及布尔津-二台构造带等次级单元（Windley et al.，2002）。该区出露的岩浆岩以中酸性岩为主，并发育有世界上最大规模伟晶岩带及其相关的Li-Nb-Ta矿产（Wang Tao et al.，2010；Dong Yu et al.，2017）。同时，该区也发育了一定数量的基性岩（Cai Keda et al.，2016），以铜镍矿化的喀拉通克超基性岩体（Han Baofu et al.，2004）最为典型。对喀拉通克基性岩体的形成背景，目前主要有后碰撞伸展环境（Wang Jingbin et al.，2006；Gao Jianfeng et al.，2012）及与晚石炭世—早二叠世地幔柱事件有关（Mao Jingwen et al.，2008；Pirajno，2010）的争议，该区基性岩的形成背景还需要更多证据支持。

科克地区位于阿尔泰山脉东段南缘、额尔齐斯断裂和可可托海-二台断裂交汇部位的西侧，为一个发育磁铁矿化的隐伏基性岩体。阿尔泰山脉东段不但发育了哈拉苏斑岩铜矿带（Xue Chunji et al.，2010），还出露有锡泊渡、喀拉通克-哈腊苏到克孜勒他乌等铜镍成矿潜力的镁铁质—超镁铁质岩带。然而，由于勘探程度的限制，目前对科克辉长岩的形成年代、岩石成因和成岩背景等科学问题认识尚不清楚，这些不足制约了对阿尔泰地区基性岩的理论认识和其相关矿产的进一步勘查工作。

本项目组前期对阿尔泰科克地区开展“典型覆盖区金属矿综合地球物理定位预测技术开发与应用”的科研项目过程中，对科克地区地球物理异常较好位置进行了钻探，勘探成果揭示该区存在隐伏辉长岩体。鉴于此，本次工作在对科克辉长岩地质特征研究基础上，进一步对该基性岩体开展了成岩年代和地球化学研究工作，据此探讨其成因，研究成果不仅对可可托海-二台断裂西侧地区的壳幔相互作

注：本文为中国地质调查局地质调查项目（编号DD20160039）资助成果。

收稿日期：2018-03-28；改回日期：2018-06-21；网络发表日期：2018-12-20；责任编辑：周健。

作者简介：张永，男，1984年生。高级工程师，矿物学、岩石学、矿床学专业。Email：yzhang027@163.com。

引用本文：张永，徐兴旺. 新疆青河县科克辉长岩体：氧化地幔楔部分熔融岩浆的记录. 2019. 地质学报，93(5)：1037～1054，doi：10.19762/j.cnki.dizhixuebao.2019046.

Zhang Yong，Xu Xingwang. 2019. The Keke gabbro in Qinghe County of Xinjiang：records from partial melting magma of the oxidized mantle wedge. Acta Geologica Sinica，93(5)：1037～1054.

用提供证据,同时也为阿尔泰地区中基性岩的时空分布、岩石成因背景及其成矿作用提供依据。

1 地质特征

1.1 区域地质背景

科克地区地处新疆阿尔泰山脉东段南缘、额尔齐斯断裂和可可托海-二台断裂交汇部位的东南侧(图 1)。新疆阿尔泰萨吾尔地区处于西伯利亚板块、哈萨克斯坦板块和天山造山带之间。阿尔泰萨吾尔地区以额尔齐斯-玛因鄂博深断裂为界与北边的阿尔泰加里东造山带接壤,南以阿尔曼泰缝合带与野马泉岛弧相接(Xue Chunji et al., 2010)。新

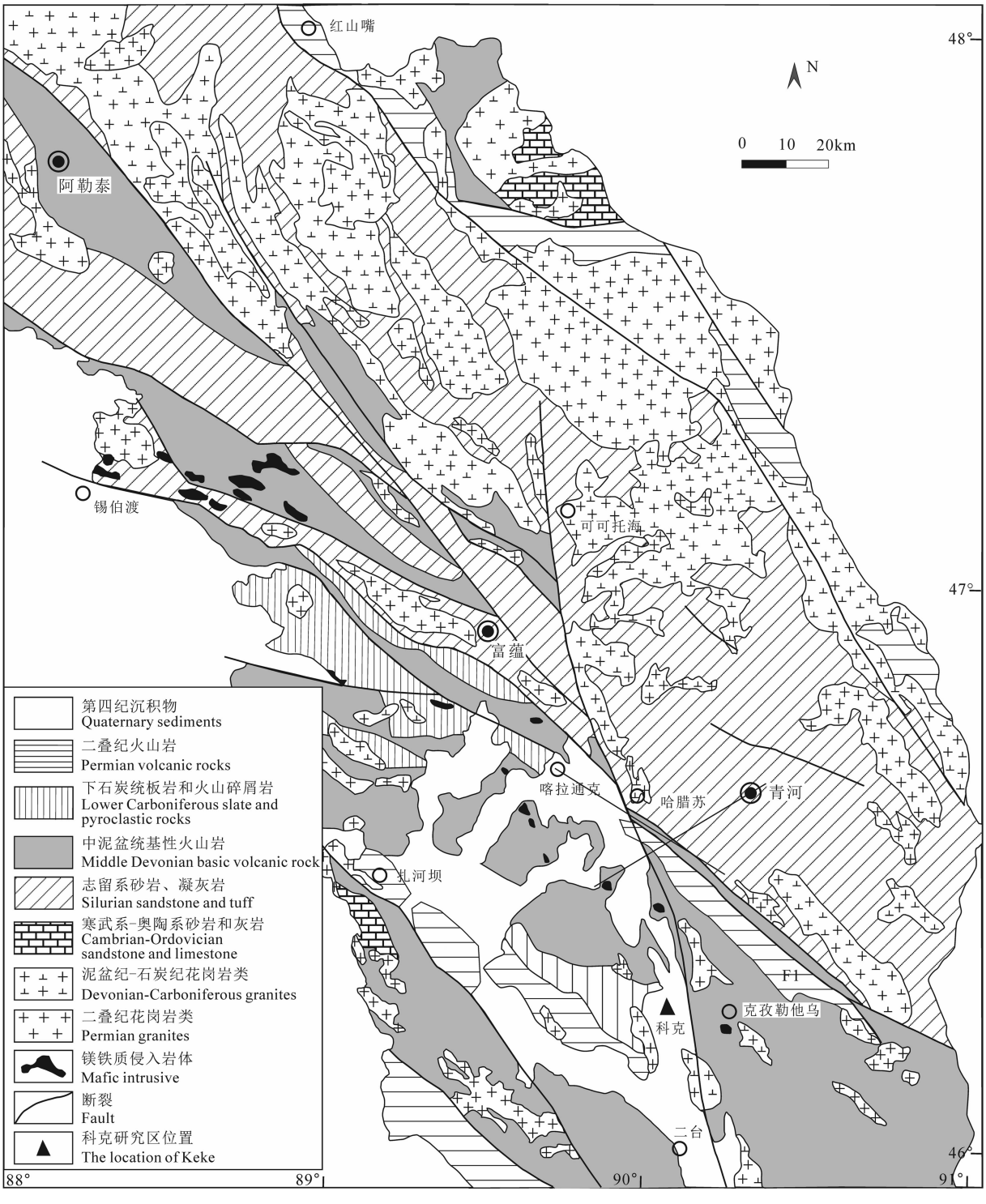

图 1 新疆青河科克地区区域地质图(据 Xue Chunji et al., 2010)

Fig. 1 Geological map of the Keke area in Qinghe, Xinjiang (after Xue Chunji et al., 2010)

疆阿尔泰科克地区出露的地层自寒武系—新生界均有分布,寒武系—奥陶系巨厚长英质细砂岩-粉砂岩构成的复理石建造、志留系砂岩凝灰岩、中泥盆统海相基性火山岩、下石炭统含碳砂板岩及火山碎屑岩、二叠纪陆相火山岩和中—新生界内陆沉积。侵入岩以额尔齐斯-玛因鄂博断裂为界,断裂北东侧大量分布,断裂南西侧出露相对较少,花岗岩的形成时代为泥盆纪—二叠纪(Wang Tao et al., 2010; Qin Kezhang et al., 2012; Jiao Jiangang et al., 2014)。值得注意的是,在额尔齐斯-玛因鄂博构造带内及其南侧发育了一条镁铁质—超镁铁质岩浆岩带(图 1),构造上处于阿尔泰地体和野马泉岛弧之间,该岩浆岩带主要赋存在泥盆系地层之中,自北西至南东具有从锡泊渡、喀拉通克经哈腊苏到克孜勒他乌均有发育,其中科克地区位于该岩浆岩带的东南端。

科克地区位于清河县萨尔托海乡北约 35km,距离青河县城 38km。该区主要为第四系砂砾石覆盖层,厚度在 50～80m 之间。前人对地球物理资料研究显示,该区具有较好的 MT 异常(Fu Chao et al., 2010),并开展了相应验证工作。科克辉长岩发现于科克地区施工的三个钻孔中,如图 2 所示。钻孔 KK01 施工深度 620m,见有多段辉长岩出现,辉长岩层的最大视厚度为 100m,钻孔 KK03 深度 710m,辉长岩出露厚度较大,钻孔 KK04 施工深度浅,辉长岩出露规模小(图 2)。钻探岩芯显示,该辉长岩侵入到泥盆系砂岩、板岩中,辉长岩体在钻孔中多以岩脉形态产出,厚大层状的岩体在深部。

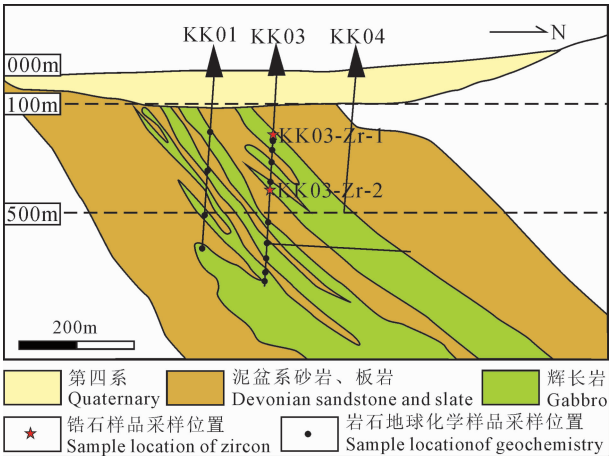

图 2　科克地区钻孔剖面地质图

Fig. 2　The geological characteristics of the drill section in Keke area

1.2　岩石学特征

钻探资料显示,科克辉长岩呈层状侵入到中泥盆统蕴都喀拉组(D_2y)砂岩、板岩地层中。辉长岩呈灰色,辉长结构,块状构造、流状构造,包含有围岩包体(图 3a,b),辉长岩主要组成矿物为斜长石、辉石、橄榄石、角闪石等,斜长石呈自形长板状或他形,杂乱分布,粒度在 0.1～0.5mm 之间,多具有聚片双晶和卡纳复合双晶;辉石呈棕褐色,为单斜辉石,自形—半自形粒状,可见有受溶蚀而呈不规则状,充填于斜长石颗粒之间,部分发生了弱的绿帘石化(图 3c,d);橄榄石呈自形粒状,星点状分布于岩石中,粒径在 0.05～0.2 mm 之间,被斜长石和单斜辉石环绕(图 3c);角闪石呈半自形粒状,星点状分布于岩石中,粒径 0.1～0.4mm。值得注意的是,辉长岩中发现有大量的磁铁矿,含量在 1 %左右,磁铁矿呈细晶—微晶状分布于斜长石、辉石颗粒之间(图 3d)。岩石遭受了后期的蚀变作用,多见有透辉石化、绿帘石化等蚀变。

2　分析测试方法

本次工作用于实验测试的辉长岩样品主要取自钻孔 KK01 和钻孔 KK03(图 2)。用于锆石 U-Pb 定年的两个辉长岩样品均取自钻孔 KK03,样品 KK03-Zr-1 取自深度 230m 处,样品 KK03-Zr-2 取自深度 484m 处,均选取新鲜的岩石。

2.1　锆石 SIMS U-Pb 同位素定年

锆石微区原位 U-Pb 同位素分析在中国科学院地质与地球物理研究所离子探针实验室完成。测试流程为:①分选:将样品破碎至矿物自然粒度后(50～150μm),通过磁选和重液等选矿技术,将矿物初步分离,然后配合双目镜手选方法进行单矿物分离提纯,分选出晶型完好、颗粒大于 50μm 的锆石(TPK-11>100 颗;TPK-05>100 颗)作为定年和成分测定对象。②制靶:在双目镜下挑选出晶形完好,透明度和色泽较好的锆石单矿物粘在载玻片的双面胶上,然后用无色透明的环氧树脂固定,待环氧树脂充分固化后,抛光至锆石颗粒露出 1/3 以上。③照相:用配有阴极发光(CL)探头的电子显微镜对锆石进行鉴定并拍照,工作电压为 15kV,电流为 4nA。这些阴极发光照片被用来检查锆石的内部结构和选择分析区域。④测年:锆石单颗粒 U-Pb 同位素测定在 CAMECA1280 离子探针仪上进行,测定结果用标准锆石 TEM 对 U、Th、Pb 含量和年龄进行了校正,实验流程和数据处理详见 Li Xianhua et al. (2009)。

2.2　全岩元素分析

科克辉长岩样品的主微量元素分析测试工作在

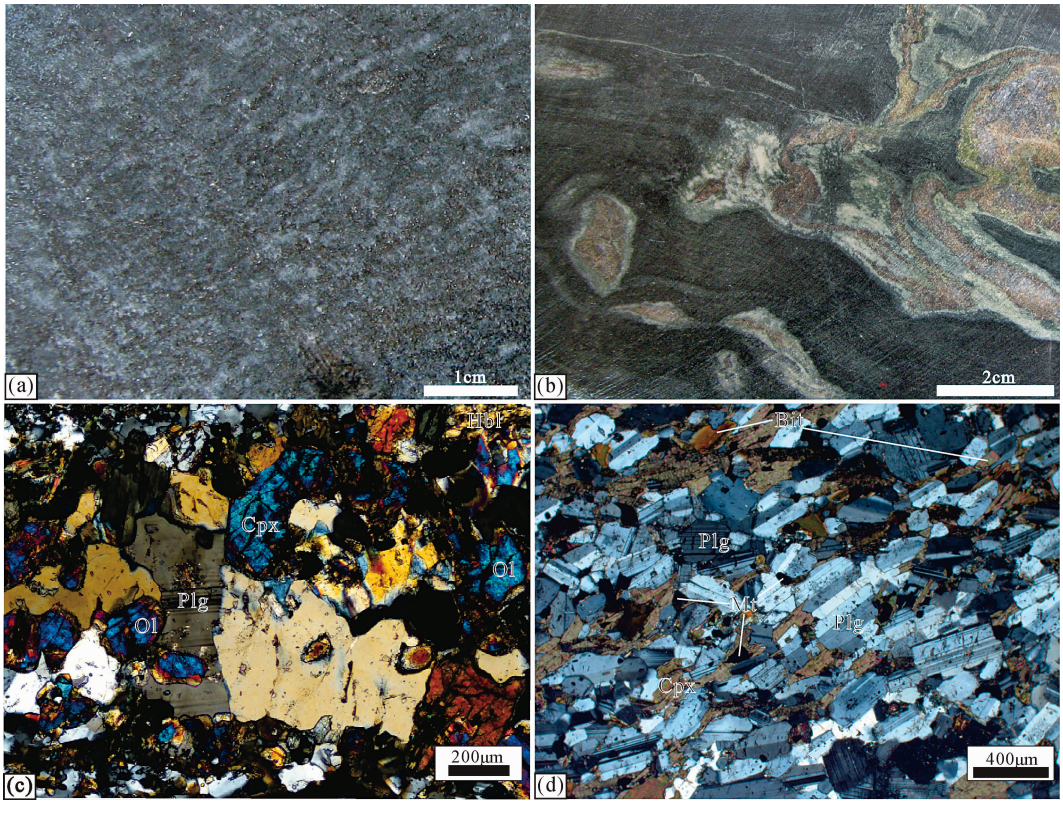

图 3 科克地区辉长岩的岩相学特征

Fig. 3 Geographical characteristics of the gabbro in Keke area

(a)—科克辉长岩;(b)—辉长岩中围岩包体;(c)、(d)—辉长岩镜下照片;
Cpx—单斜辉石;Plg—斜长石;Ol—橄榄石;Hbl—角闪石;Bit—黑云母;Mt—磁铁矿

(a)—Keke gabbro;(b)—enclaves in gabbro;(c), (d)—photomicrograph;
Cpx—clinopyroxene; Plg—plagioclase; Ol—olivine; Hbl—hornblende; Bit—biotite; Mt—magnetite

中国科学院地质与地球物理研究所岩石圈演化国家重点实验室完成。主量元素的分析测试方法为:①先将岩石样品制成粒度不大于 200 目的粉末,后用烘箱(约 100℃)干燥,最后在高温炉(>1000℃)中持续灼烧 2 h,最后测得其烧失量(LOI);② 取 4 g $Li_2B_4O_7$ 溶液和①步骤后所得的 0.5 g 粉末样品一起混匀放置于塑料瓶中,在 XRF 专门的铂金坩埚中先加入 0.4g 1% LiBr 和 0.5%助熔剂 NH_4I,后加入混合样品,在 1250℃熔融,制备成 XRF 测定用的玻璃饼。微量、稀土元素的分析测试方法为:①先将岩石样品制成粒度不大于 200 目的粉末,在已有 2 mL 8 mol HNO_3 和 0.5 mL 8 mol HF 熔样罐中加入粉末,用电热板(约 100℃)加热直至让样品充分溶解;②在通风橱中开启熔样罐蒸干样品并且在蒸干后再次倒入 2 mL 8 mol HNO_3 同时加热,方法和前面一致;③利用去离子水,稀释 8 mol HNO_3 溶解的样品溶液至 250 ml,然后在溶样瓶中摇均匀后将 10mL 溶液放入细小塑料管,备 ICPMS 测试,样品测试采用内标法。具体的分析流程参见 Li Xianhua et al.(2002)。

3 分析结果

3.1 锆石 SIMS U-Pb 同位素测年

本次工作测得科克地区辉长岩体 2 个样品(KK03-Zr-1 和 KK03-Zr-2)的锆石 SIMS U-Pb 年龄结果如表 1 和图 4 所示。两个样品的锆石颗粒均较小,多数锆石的长度和宽度均小于 100μm。样品 KK03-Zr-1 的锆石颗粒多成不规则状,部分呈长柱状,阴极发光图像总体亮度较高,可能跟锆石中 U 含量较低有关,除锆石 KK03-Zr-1-12 和 KK03-Zr-1-13 中的 U 含量分别为 1431×10^{-6}、1981×10^{-6} 之外,其余 14 颗锆石的 U 含量在 89×10^{-6}～576×10^{-6} 之间,锆石 KK03-Zr-1-1、KK03-Zr-1-2、KK03-Zr-1-3、KK03-Zr-1-12、KK03-Zr-1-13 五颗锆石阴极发光图像颜色明显较暗。对样品 KK03-Zr-1 中的 16 颗锆石进行了测年分析,结果(表 1)显示,$^{206}Pb/^{238}U$ 年龄值在 278.6～2547.4Ma 之间,11 颗锆石 $^{206}Pb/^{238}U$ 年龄值在 278.6～303.7Ma 之间。且其谐和年龄值为 290.8±3.5Ma。其中有 5 颗锆

表 1　科克地区钻孔辉长岩 SIMS 锆石 U-Pb 年龄数据

Table 1　SIMS zircon U-Pb age data for gabbro in the Keke area

测年点号	($\times10^{-6}$)		U/Th	同位素比值						年龄(Ma)					
	^{232}Th	^{238}U		$^{207}Pb/^{206}Pb$	1δ	$^{207}Pb/^{235}U$	1δ	$^{206}Pb/^{238}U$	1δ	$^{207}Pb/^{206}Pb$	1δ	$^{207}Pb/^{235}U$	1δ	$^{206}Pb/^{238}U$	1δ
KK03-Zr-1-1	238	170	0.71	1.0730	0.020	0.1213	0.015	0.0641	0.013	746.4	27.1	740.1	10.5	738.0	10.5
KK03-Zr-1-2	576	201	0.35	11.3180	0.015	0.4966	0.015	0.1653	0.003	2510.5	4.4	2549.7	14.4	2599.2	32.3
KK03-Zr-1-3	299	311	1.04	11.6640	0.016	0.5007	0.015	0.1690	0.004	2547.4	6.3	2577.8	14.6	2616.7	32.3
KK03-Zr-1-4	108	49	0.45	0.3340	0.038	0.0464	0.019	0.0522	0.033	294.3	72.9	292.3	9.6	292.1	5.3
KK03-Zr-1-5	116	25	0.22	0.3500	0.043	0.0466	0.017	0.0544	0.040	386.8	86.9	304.5	11.4	293.8	4.8
KK03-Zr-1-6	192	174	0.90	1.0510	0.023	0.1198	0.015	0.0636	0.018	729.5	36.9	729.3	12.1	729.2	10.4
KK03-Zr-1-7	163	132	0.81	1.0920	0.022	0.1224	0.015	0.0647	0.016	765.5	33.3	749.7	11.7	744.4	10.6
KK03-Zr-1-8	89	15	0.17	0.3170	0.071	0.0442	0.015	0.0520	0.069	286.5	150.6	279.5	17.4	278.6	4.2
KK03-Zr-1-9	278	222	0.80	0.3360	0.033	0.0454	0.015	0.0537	0.030	359.0	65.8	294.1	8.6	286.0	4.3
KK03-Zr-1-10	348	341	0.98	0.3360	0.030	0.0463	0.015	0.0526	0.027	311.3	59.2	294.1	7.8	292.0	4.3
KK03-Zr-1-11	414	369	0.89	0.3190	0.024	0.0444	0.016	0.0521	0.018	288.2	40.9	280.9	5.9	280.0	4.2
KK03-Zr-1-12	1431	594	0.42	0.3410	0.017	0.0467	0.015	0.0529	0.009	326.3	19.2	297.9	4.5	294.3	4.3
KK03-Zr-1-13	1981	2067	1.04	0.3340	0.019	0.0468	0.015	0.0519	0.011	279.4	25.5	292.9	4.8	294.6	4.3
KK03-Zr-1-14	462	261	0.57	0.3480	0.022	0.0482	0.015	0.0523	0.016	296.7	36.8	302.9	5.8	303.7	4.5
KK03-Zr-1-15	378	160	0.42	0.3320	0.023	0.0460	0.015	0.0523	0.017	299.8	37.5	291.2	5.7	290.1	4.3
KK03-Zr-1-16	154	80	0.52	0.3400	0.030	0.0470	0.016	0.0524	0.025	303.2	56.7	296.9	7.8	296.1	4.7
KK03-Zr-2-1	432	8	0.02	0.7120	0.019	0.0863	0.015	0.0599	0.010	599.0	22.1	546.0	7.8	533.4	7.9
KK03-Zr-2-2	378	93	0.25	0.3460	0.024	0.0484	0.015	0.0519	0.019	281.7	42.8	301.8	6.3	304.4	4.5
KK03-Zr-2-3	1362	633	0.47	0.3370	0.017	0.0467	0.015	0.0524	0.008	302.8	17.0	295.2	4.4	294.2	4.4
KK03-Zr-2-4	69	61	0.88	10.1710	0.018	0.4600	0.015	0.1604	0.009	2459.4	15.4	2450.4	16.6	2439.7	31.0
KK03-Zr-2-5	1325	564	0.43	0.3440	0.017	0.0467	0.015	0.0534	0.007	347.2	15.2	300.3	4.3	294.3	4.4
KK03-Zr-2-6	241	122	0.51	11.6460	0.017	0.5084	0.016	0.1662	0.006	2519.3	9.9	2576.4	16.1	2649.7	34.9
KK03-Zr-2-7	2173	581	0.27	0.3540	0.017	0.0495	0.016	0.0518	0.005	277.8	11.8	307.4	4.4	311.3	4.8
KK03-Zr-2-8	221	91	0.41	0.2980	0.035	0.0423	0.015	0.0511	0.032	246.6	71.4	265.0	8.2	267.1	3.9
KK03-Zr-2-9	1339	508	0.38	0.3510	0.018	0.0482	0.015	0.0527	0.010	317.6	21.6	305.2	4.7	303.6	4.5
KK03-Zr-2-10	969	265	0.27	0.3570	0.017	0.0498	0.015	0.0521	0.008	288.3	17.8	310.2	4.6	313.1	4.6
KK03-Zr-2-11	459	112	0.24	0.3420	0.021	0.0484	0.016	0.0512	0.013	251.3	29.9	298.8	5.3	304.9	4.7
KK03-Zr-2-12	403	95	0.24	0.3390	0.020	0.0482	0.015	0.0510	0.013	243.1	30.7	296.8	5.2	303.6	4.5
KK03-Zr-2-13	2269	829	0.37	0.3640	0.018	0.0505	0.015	0.0523	0.008	299.8	19.1	315.5	4.7	317.7	4.7
KK03-Zr-2-14	2609	558	0.21	0.3290	0.017	0.0450	0.016	0.0530	0.006	329.2	12.4	288.7	4.3	283.7	4.5
KK03-Zr-2-15	259	193	0.75	5.5180	0.016	0.3387	0.015	0.1182	0.006	1928.8	10.9	1903.4	14.0	1880.2	24.5
KK03-Zr-2-16	305	140	0.46	0.7890	0.039	0.0957	0.032	0.0598	0.023	597.2	48.5	590.7	17.8	589.0	18.1
KK03-Zr-2-17	1035	349	0.34	0.3590	0.018	0.0500	0.015	0.0521	0.009	288.8	20.8	311.4	4.7	314.4	4.6
KK03-Zr-2-18	1180	315	0.27	0.3020	0.020	0.0411	0.015	0.0534	0.013	345.6	28.1	268.2	4.7	259.4	3.9
KK03-Zr-2-19	2399	1159	0.48	0.3320	0.016	0.0458	0.015	0.0526	0.007	309.9	14.6	291.1	4.1	288.8	4.2
KK03-Zr-2-20	1030	395	0.38	0.3190	0.020	0.0433	0.015	0.0535	0.013	348.8	27.9	281.4	4.8	273.3	4.0
KK03-Zr-2-21	1760	828	0.47	0.3450	0.017	0.0481	0.015	0.0521	0.009	291.1	19.6	301.3	4.5	302.7	4.4
KK03-Zr-2-22	895	300	0.34	0.3370	0.019	0.0476	0.015	0.0514	0.011	257.3	25.3	295.2	4.8	300.0	4.4
KK03-Zr-2-23	2704	1153	0.43	0.3500	0.016	0.0490	0.015	0.0518	0.006	277.2	13.6	304.7	4.3	308.3	4.5
KK03-Zr-2-24	799	264	0.33	0.3260	0.020	0.0453	0.015	0.0523	0.013	297.9	28.4	286.7	4.9	285.4	4.2
KK03-Zr-2-26	1155	489	0.42	0.3210	0.018	0.0445	0.015	0.0523	0.010	300.4	23.4	282.7	4.5	280.6	4.2
KK03-Zr-2-27	1434	753	0.53	0.3360	0.018	0.0464	0.015	0.0525	0.010	306.9	22.3	294.0	4.7	292.4	4.4
KK03-Zr-2-28	963	259	0.27	0.3370	0.019	0.0466	0.015	0.0525	0.012	306.0	26.9	295.2	4.9	293.8	4.3

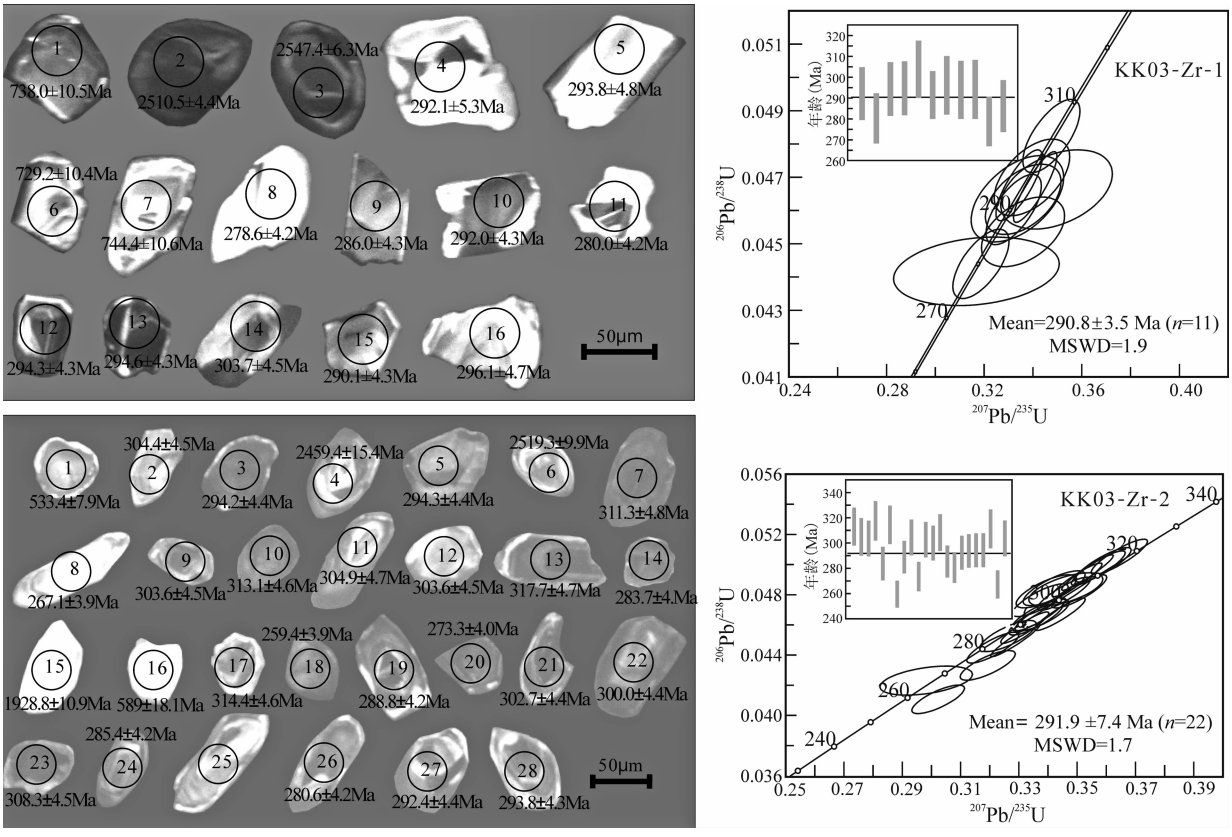

图 4 科克辉长岩 KK03-Zr-1 和 KK03-Zr-2 样品的锆石 U-Pb 年龄谐和图

Fig. 4 Zircon U-Pb concordia diagrams of the samples KK03-Zr-1 and KK03-Zr-2 of gabbro from Keke area

石(KK03-Zr-1-1、K03-Zr-1-2、KK03-Zr-1-3、KK03-Zr-1-6 和 KK03-Zr-1-7)的年龄值较老,分别是 738.0±10.5Ma ($^{206}Pb/^{238}U$年龄)、2510.5±4.4Ma ($^{207}Pb/^{206}Pb$ 年龄)、2547.4±6.3Ma ($^{207}Pb/^{206}Pb$ 年龄)、729.2±10.4Ma ($^{206}Pb/^{238}U$ 年龄)和 744.4±10.6Ma ($^{206}Pb/^{238}U$ 年龄),结合锆石的阴极发光图像,这 5 颗锆石早于辉长岩的形成时代,应属辉长岩的捕获锆石。

对样品 KK03-Zr-2 的 28 颗锆石进行了 28 个分析测试点,获得了 27 组有效数据,锆石分析点 KK03-Zr-2-25 的 f_{206} 值为 1.97%(f_{206} 指示了普通铅在总铅中的含量,值越小表示测试精确越高),测试精度低于标准,故该分析值不能使用。阴极发光图像显示,9 颗锆石(KK03-Zr-2-1、KK03-Zr-2-2、KK03-Zr-2-4、KK03-Zr-2-6、KK03-Zr-2-8、KK03-Zr-2-11、KK03-Zr-2-12、KK03-Zr-2-15、KK03-Zr-2-16)图像较亮,由其含有较低 U($69\times10^{-6}\sim459\times10^{-6}$)和 Th($8\times10^{-6}\sim193\times10^{-6}$)含量导致。测年结果(表 1)显示,$^{206}Pb/^{238}U$ 年龄值在 278.6~2519.3Ma 之间,其中 22 颗锆石的 $^{206}Pb/^{238}U$ 年龄集中在 259.4~317.7Ma 之间,$^{206}Pb/^{238}U$ 年龄进行加权平均得到 291.9±7.4Ma 年龄值。其他五颗锆石(KK03-Zr-2-1、KK03-Zr-2-4、KK03-Zr-2-6、K03-Zr-2-15、KK03-Zr-2-16)年龄值较老(分别为 533.4±7.9Ma、2459.4±15.4Ma、2519.3±9.9Ma、1928.8±10.9Ma 和 589±18.1Ma),他们均呈浑圆状、岩浆振荡环带不清晰,显示了继承锆石或捕获锆石的特征。

3.2 辉长岩地球化学特征

科克辉长岩的元素地球化学特征如表 2 所示。该辉长岩体 12 个样品的 SiO_2 含量在 46.14%~52.53%之间,平均 50.23%;TiO_2 为 0.78%~1.13%,平均 0.91%;Al_2O_3 为 13.82%~19.44%,平均 16.50%;TFe_2O_3 为 12.06%~15.68%,平均 13.56%;MgO 为 3%~7.68%,平均 5.35%;CaO 为 3.17%~12.42%,平均 7.45%;(Na_2O+K_2O)含量为 2.17%~8.21%,平均 5.15%;其中 K_2O 含量为 0.21%~3.39%,P_2O_5 为 0.13%~0.31%。$Mg^{\#}$ 介于 33.03~56.79 之间,平均值为 46.85。在地球化学判别图解上,科克辉长岩投点于辉长岩-碱性辉长岩区域(图 5a),具有低钾—高钾岩石序列特点(图 5b)。

表 2　科克地区辉长岩主量元素(%)和微量元素($\times10^{-6}$)组成

Table 2　The major (%) and trace ($\times10^{-6}$) elements compositions for gabbro in the Keke area

样品号	KK01-4	KK01-5	KK01-9	KK01-20	KK03-2	KK03-4	KK03-5	KK03-9	KK03-13	KK03-24	KK03-26	KK03-34
岩性	辉长岩	辉长岩	辉长岩	辉长岩	辉长岩	辉长岩	辉长岩	辉长岩	辉长岩	辉长岩	辉长岩	辉长岩
SiO_2	50.03	48.34	46.14	47.31	50.51	52.53	52.04	51.03	51.07	52.02	51.69	50.01
TiO_2	0.82	0.95	1.13	0.87	1.01	0.91	0.94	0.78	0.82	0.82	0.95	0.92
Al_2O_3	17.67	16.43	19.44	18.04	15.55	13.82	14.61	16.20	15.31	15.83	16.13	18.95
TFe_2O_3	12.52	13.71	13.49	13.62	14.64	13.85	14.35	12.22	12.41	12.06	15.68	14.19
MnO	0.17	0.19	0.24	0.21	0.22	0.26	0.26	0.19	0.18	0.21	0.20	0.14
MgO	5.44	3.81	3.47	7.68	3.92	7.63	7.12	6.79	6.25	5.40	3.72	3.00
CaO	6.30	10.71	12.42	3.17	11.47	6.68	7.85	5.33	7.00	6.28	6.72	5.42
Na_2O	5.54	4.43	0.65	4.82	0.01	0.21	0.38	5.06	5.71	5.27	3.45	4.36
K_2O	1.38	0.79	2.48	3.39	2.16	2.44	2.01	2.25	0.21	1.11	1.16	2.54
P_2O_5	0.23	0.28	0.31	0.18	0.21	0.17	0.20	0.18	0.13	0.17	0.20	0.22
LOI	0.26	0.17	0.02	0.50	0.31	1.22	0.47	0.24	0.63	0.24	0.03	0.32
TOTAL	100.36	99.82	99.79	99.79	100.00	99.72	100.23	100.27	99.72	99.41	99.92	100.08
$Mg^{\#}$	50.30	39.30	37.40	56.80	38.40	56.20	53.60	56.40	54.00	51.10	35.60	33.00
Li	35.00	11.23	9.65	37.01	30.83	57.08	40.40	28.88	18.72	31.19	8.12	43.28
Be	0.63	0.53	0.65	0.24	0.72	0.59	0.62	0.53	0.60	0.55	0.63	0.52
Sc	38.64	43.38	52.39	41.13	47.04	41.16	44.98	41.15	41.97	39.81	43.85	41.89
V	342.33	408.29	535.78	420.09	450.89	404.61	448.85	323.50	383.01	351.44	428.54	339.09
Cr	46.12	43.63	74.13	37.38	51.99	26.10	46.63	60.05	38.78	48.54	53.01	46.95
Co	33.45	37.72	35.52	38.33	34.14	35.78	39.95	34.54	35.00	34.68	40.87	42.03
Ni	12.73	12.92	13.10	10.04	9.20	9.99	12.65	18.30	18.98	9.93	13.46	15.30
Cu	158.07	175.15	246.45	38.17	195.64	126.86	175.82	150.64	128.25	107.06	216.23	154.07
Zn	86.87	112.55	93.10	96.00	101.58	103.61	113.81	90.09	88.19	98.25	139.44	143.30
Ga	16.50	16.49	19.89	18.66	17.86	15.95	17.52	15.64	16.42	15.71	17.92	19.47
Rb	15.83	3.39	25.39	56.88	29.70	37.52	30.62	15.05	2.41	20.80	17.33	37.61
Sr	1069.33	402.71	300.77	202.82	169.41	126.24	225.04	405.61	302.52	692.41	323.29	231.82
Y	18.99	18.96	22.34	10.50	23.39	21.47	23.38	19.29	17.37	19.97	25.49	22.48
Zr	68.85	74.10	84.81	22.44	82.80	75.23	79.79	62.68	67.84	68.15	75.15	81.09
Nb	2.84	3.21	3.23	2.20	2.41	2.26	2.34	2.07	2.16	2.26	2.22	2.53
Cs	2.53	0.08	1.70	14.56	3.68	6.50	4.99	2.30	0.44	2.75	1.84	1.98
Ba	294.44	248.02	970.69	660.50	133.16	324.71	297.16	925.42	189.81	453.56	101.57	211.46
Hf	2.12	2.21	2.49	0.75	2.57	2.37	2.47	1.95	2.10	2.16	2.30	2.57
Ta	0.14	0.14	0.15	0.10	0.13	0.12	0.12	0.10	0.10	0.11	0.11	0.14
Tl	0.13	0.04	0.11	0.14	0.10	0.13	0.12	0.09	0.04	0.08	0.08	0.14
Pb	7.51	6.45	5.78	2.44	5.15	6.85	6.73	3.60	4.46	3.71	2.85	4.59
Bi	0.03	0.03	0.02	0.02	0.03	0.03	0.03	0.03	0.03	0.02	0.05	0.02
Th	1.86	1.71	1.61	0.51	1.43	1.36	1.51	1.14	1.17	1.59	1.32	0.98
U	0.77	0.72	0.70	0.16	0.67	0.57	0.69	0.56	0.51	0.78	0.59	0.55
La	15.43	17.15	16.73	11.43	10.85	11.08	11.65	9.29	9.33	10.41	11.51	13.46
Ce	31.17	33.36	34.35	21.75	24.76	23.82	24.61	19.72	19.70	22.32	24.76	27.31
Pr	4.30	4.57	4.87	3.07	3.72	3.43	3.85	3.17	2.90	3.42	3.87	3.94
Nd	18.70	18.98	21.51	13.09	16.69	15.80	16.65	14.56	13.75	15.97	16.79	17.20
Sm	4.26	4.26	5.01	2.79	4.24	3.83	4.12	3.49	3.36	3.88	4.29	3.91
Eu	1.26	1.18	1.75	1.18	1.27	1.22	1.35	1.29	0.94	1.20	1.17	1.18
Gd	3.57	3.71	4.21	2.41	3.44	3.25	3.44	3.08	2.86	3.29	3.71	3.32
Tb	0.58	0.59	0.68	0.36	0.63	0.58	0.63	0.55	0.50	0.59	0.68	0.60
Dy	3.63	3.59	4.18	2.12	4.16	3.88	4.28	3.61	3.29	3.76	4.55	3.96
Ho	0.74	0.72	0.86	0.40	0.90	0.83	0.91	0.76	0.70	0.79	0.96	0.85
Er	2.00	1.96	2.38	1.08	2.44	2.29	2.59	2.08	1.99	2.16	2.66	2.36
Tm	0.30	0.29	0.36	0.15	0.36	0.35	0.39	0.32	0.29	0.33	0.39	0.36
Yb	1.86	1.90	2.33	0.91	2.30	2.22	2.54	2.06	1.92	2.13	2.46	2.28
Lu	0.29	0.29	0.35	0.14	0.36	0.34	0.39	0.32	0.30	0.32	0.37	0.34
ΣREE	88.09	92.54	99.57	60.86	76.13	72.93	77.40	64.28	61.84	70.58	78.16	81.06
δEu	0.99	0.91	1.16	1.39	1.02	1.06	1.09	1.20	0.93	1.02	0.90	1.00
$(La/Yb)_N$	5.95	6.48	5.14	9.06	3.38	3.58	3.29	3.24	3.48	3.50	3.35	4.24
LREE	73.85	78.31	82.47	52.12	60.26	57.96	60.88	50.23	49.04	56.00	61.21	65.81
HREE	12.97	13.04	15.35	7.57	14.59	13.74	15.17	12.77	11.85	13.38	15.78	14.07
δCe	0.94	0.92	0.93	0.90	0.96	0.95	0.90	0.89	0.93	0.92	0.91	0.92

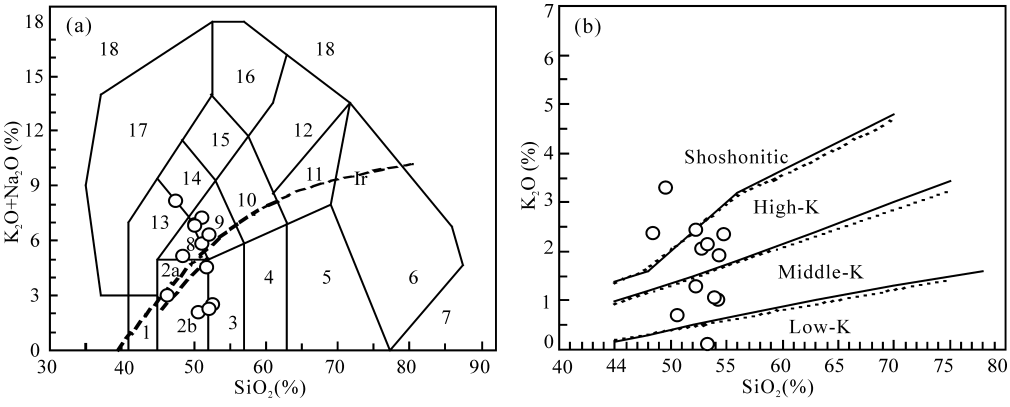

图 5 科克辉长岩体的岩性判别图解

Fig. 5 Classification of the Keke gabbro using major and trace elements

(a)—侵入岩 TAS 图解(底图据 Middlemost,1994);1—橄榄辉长岩;2a—碱性辉长岩;2b—亚碱性辉长岩;3—辉长闪长岩;4—闪长岩;5—花岗闪长岩;6—花岗岩;7—硅英岩;8—二长辉长岩;9—二长闪长岩;10—二长岩;11—石英二长岩;12—正长岩;13—副长石辉长岩;14—副长石二长闪长岩;15—副长石二长正长岩;16—副长正长岩;17—副长深成岩;18—霓方钠岩-磷霞岩-白榴岩;Ir—Irvine 分界线,上方为碱性,下方为亚碱性;(b)—K_2O-SiO_2 图解(底图据 Ewart,1982)

(a)—TAS plot for plutonic rocks (after Middlemost,1994); 1—olivine gabbro; 2a—alkali-gabbro; 2b—sub-alkali-gabbro; 3—gabbro-diorite; 4—diorite; 5—granodiorite; 6—granite; 7—quartzolite; 8—monzogabbro; 9—monzodiorite; 10—monzonite; 11—quartz monzonite; 12—syenite; 13—vice-feldspar gabbro; 14—vice-feldspar monzonite diorite; 15—vice-feldspar syenite monzonite; 16—mate syenite; 17—mate plutonic; 18—tawite /urtite /leucitite; Ir—Irvine dividing line, above is alkaline, below the sub-alkaline. (b)—K_2O vs. SiO_2 plot (after Ewart, 1982)

科克辉长岩体的哈克图解(图 6)显示,随着 MgO 减小,具有 Al_2O_3、CaO、P_2O_5 含量增高,SiO_2、TiO_2、TFeO 和全碱含量(K_2O+Na_2O)含量变化不显著的特点,科克辉长岩具有较低的烧失量,其 LOI 值在 0.02～1.22 之间(图 6i)。

科克辉长岩的稀土总量集中在 60.86×10^{-6}～99.57×10^{-6} 之间,均值 79.65×10^{-6};轻稀土和重稀土元素比值(LREE/HREE)在 3.88～6.89 之间,均值为 4.76;δEu 值在 0.90～1.39,均值为 1.06;除样品 KK01-20 有较高 $(La/Yb)_N$ 值(9.06)之外,其他样品 $(La/Yb)_N$ 值在 3.24～6.48 之间,均值 4.15。稀土元素球粒陨石标准化配分曲线图(图 7a)显示科克辉长岩具有轻稀土富集、重稀土亏损的右倾特征,但轻重稀土分馏不明显,δEu 值呈弱正异常特征,微量元素蛛网图(图 7b)显示,科克辉长岩具有 Ba、K、Y 富集,Th、Nb、Ta、Ti 亏损的特点,表现为大离子亲石元素(LILE)含量高于高场强元素(HFSE)。微量稀土元素标准化蛛网图显示,科克辉长岩体与喀拉通克岩体具有相似特征,而与攀枝花岩体明显不同(图 7a, b)。

4 讨论

4.1 成岩年代

本文科克地区辉长岩体两个样品(KK03-Zr-1 和 KK03-Zr-2)的锆石 $^{206}Pb/^{238}U$ 年龄值分别为 290.8±3.5Ma($n=11$, MSWD=1.9)和 291.9±7.4Ma($n=22$, MSWD=1.7),两者在误差范围内一致,指示了科克辉长岩体形成于 291Ma 左右,属早二叠世。

前人对阿尔泰造山带地区中基性岩的形成年代做了较多研究工作。Han Baofu et al.(2004)测得喀拉通克 1 号辉长岩岩体的锆石 SHRIMP 年龄为 287±5Ma;Jiao Jiangang et al.(2014)测得喀拉通克 Y9 岩体的 SHRIMP 年龄为 287±4Ma;Y1 和 Y2 号岩体中铜镍硫化物矿石的 Re-Os 同位素等时线年龄分别为 282.5Ma 和 290.2Ma(Zhang Zuoheng et al., 2005;Han Chunming et al., 2006)。Liu Fei et al.(2013)研究认为,额尔齐斯断裂带左行走滑剪切带的主期活动时限为 292～274Ma。本文测得科克地区辉长岩为 291Ma,指示为锡泊渡—喀拉通克经哈腊苏—克孜勒他乌基性岩带的重要组成部分。

近年来,北疆地区与基性岩相关的铜镍矿床陆续报道,如表 3 所示,是该区的找矿勘探的重点方向之一,这些基性岩体广泛分布在塔里木北缘(坡一、坡十、坡北)、东天山(黄山、黄山东、镜儿泉、香山、白石泉、图拉尔根等)和阿尔泰地区(喀拉通克等),这些铜镍矿化基性岩体均形成于早二叠世(Xue Shengchao et al., 2016;Zhou Taofa et al., 2010)。

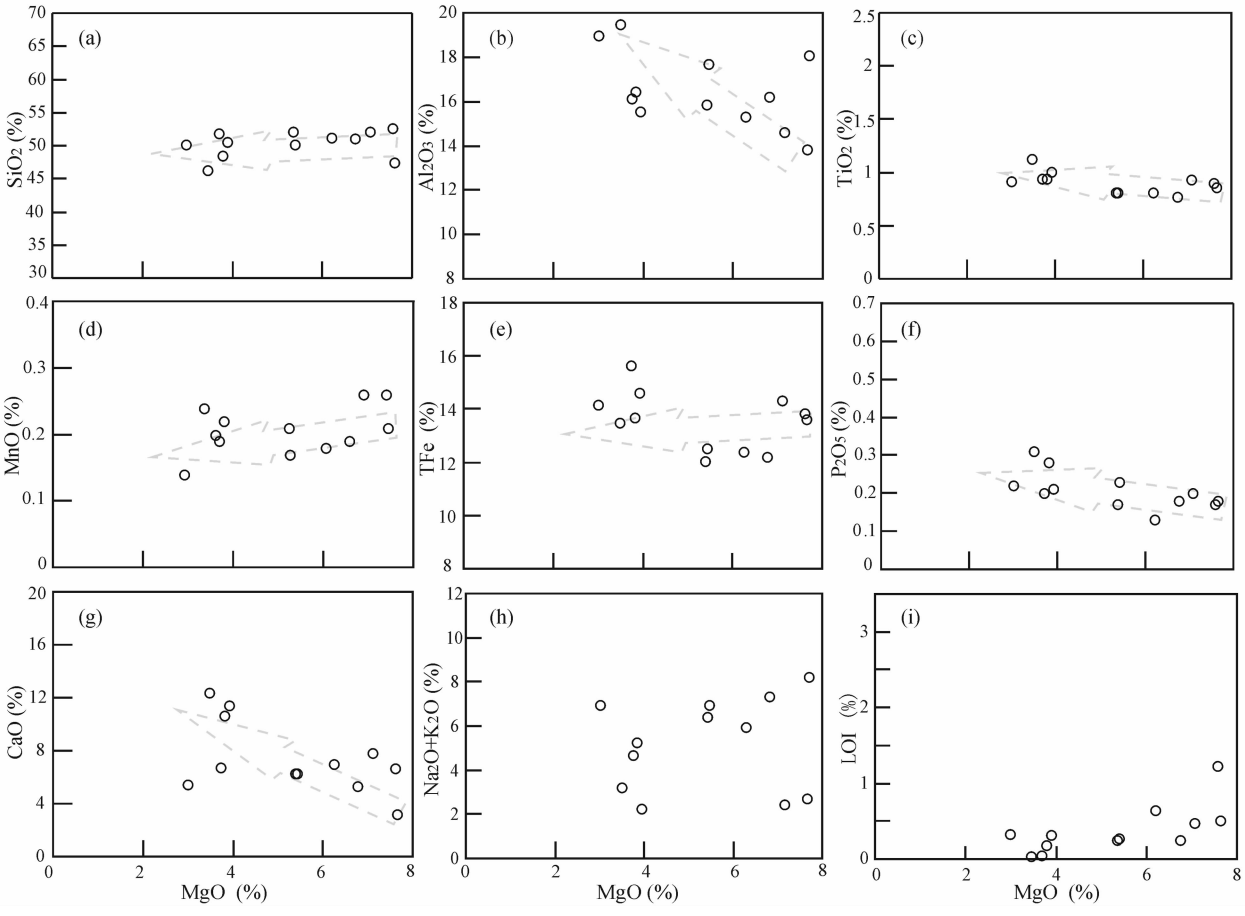

图 6　科克辉长岩体的主量元素 Hark 图解

Fig. 6　Hark diagram of the Keke gabbro using major elements

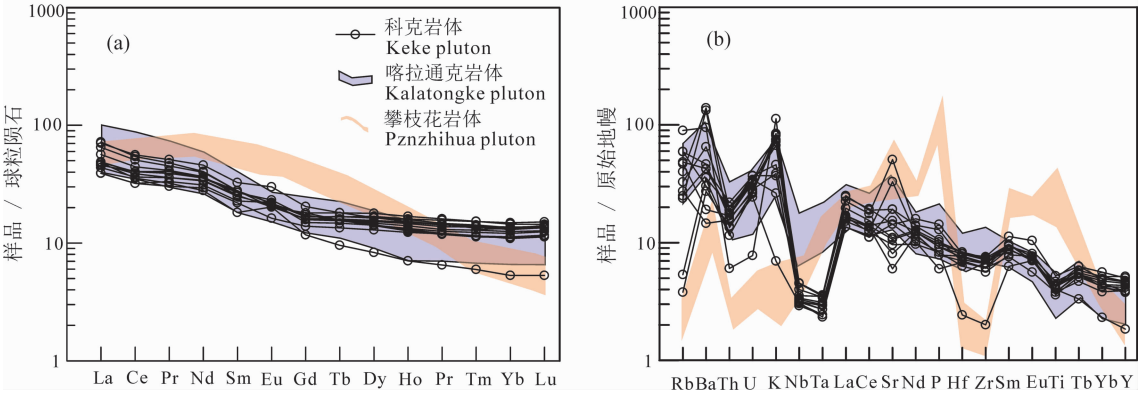

图 7　科克辉长岩的球粒陨石标准化稀土元素配分曲线(a)(球粒陨石标准值据 Taylor and McLennan, 1985)和原始地幔标准化微量元素蛛网图(b)(原始地幔标准值据 Sun and McDonough, 1989)

Fig. 7　Chondrite standardized REE diagram (a) (after Taylor and McLennan, 1985) and primitive mantle standardized trace elements spider diagrams (b) (after Sun and McDonough, 1989) of the gabbro in Keke area

数据来源:喀拉通克据 Jiang Changyi et al. (2009);攀枝花据 Hu Xiaoqin et al. (2016);科克据本文

Data from: Kalatongke after Jiang Changyi et al. (2009); Panzhihua after Hu Xiaoqin et al. (2016); Keke after this paper

本次研究的科克辉长岩侵位于下二叠统,与邻近的喀拉通克岩体的成岩时代一致(表 3),且与北疆大规模分布的铜镍硫化物矿化基性岩具有一致的时空分布特点。

4.2　岩石成因

在基性岩石中,高场强元素(HFSE)包括 Th、

表 3 新疆北部地区基性岩年代表

Table 3 The reported mafic intrusions age in northern Xinjiang region

地区	名称	岩性	测年方法	年龄(Ma)	资料来源
阿尔泰	科克	辉长岩	锆石 LA-ICP-MS	290.8±3.5 291.4±5.0	本文
	喀拉通克	(阿尔泰南)喀拉通克 1 号岩体	锆石 SHRIMP	287±5	Jiao Jiangang et al., 2014
			Re-Os 等时线	282.5±4.8 290.2±6.9	Zhang Zuoheng et al., 2005
东天山	黄山	辉橄岩	锆石 SHRIMP	283.8±3.4	Qin Kezhang et al.,2011
		闪长岩	SHRIMP 锆石 U-Pb	269±2	Zhou Meifu et al., 2004
	黄山东	铜、镍硫化物矿石	Re-Os	282±20	Mao Jingwen et al., 2002
		块状—浸染状矿石	Sm-Nd	320 ±38	Li Huaqin et al., 1998
		黄山东岩体	锆石 SHRIMP	274 ± 3	Han Baofu et al., 2004
	香山	块状—浸染状矿石	Re-Os	298±7.1	Li Yuechen et al., 2006
		基性—超基性岩	Rb-Sr	285	Li Huaqin et al., 1998
		基性—超基性岩	单颗粒锆石 U-Pb	286±12	Qin Kezhang et al., 2000
			SHRIMP 锆石 U-Pb	285±1.2	Qin Kezhang et al., 2002
	白石泉	辉橄岩、橄辉岩、辉石岩	锆石 LA-ICP-MS	284	Wu Hua et al., 2005
			锆石 LA-ICP-MS	281.2±0.9	Mao Qigui et al., 2008
	葫芦	基性—超基性岩	Re-Os	283±13	Chen Shiping et al., 2005
	天宇	橄辉岩及辉石岩	Re-Os	835±210	Wang Hong, 2007
			锆石 LA-ICP-MS	290.2±3.4	Tang Dongmei et al., 2009
	土墩	角闪橄榄岩、角闪辉长眼、苏长岩	K-Ar	240	Wang Runmin et al., 1987
	镜儿泉	橄榄岩、辉石岩		260.2	Gu Lianxing et al., 2006
	四顶黑山	层状超基性岩体	Ar-Ar	545	Xu Xinwang et al., 2006
	十里坡	玄武岩	锆石 LA-ICP-MS	309	Zhang Dayu et al., 2012
	东尖峰	玄武岩	锆石 SHRIMP	306	Zhang Dayu et al., 2012
	尾亚	钒钛磁铁矿基性岩	单颗粒锆石 U-Pb	257.8,260.1	Wang Yuwang et al., 2007
塔里木北缘	坡北	(北山地块内,星星峡)基性超基性岩体(辉长岩)	Sm-Nd	307 ±32	Li Huaqin et al., 2009
			锆石 SHRIMP	278±2	Li Huaqin et al., 2009
		坡北十号岩体	锆石 SHRIMP	289±13	Li Huaqin et al., 2009
	坡一	北山裂谷 基性超基性岩体	锆石 SHRIMP	278±2	Li Huaqin et al., 2009
	坡十	北山裂谷 基性超基性岩体	锆石 SHRIMP	274±4	Jiang Changyi et al., 2006

Ti、Nb、Ta、Zr、Hf、Y 以及稀土元素(REE)在岩石中比较稳定,不容易受到后期热液作用影响(Winchester et al., 1976; Barley et al., 2000; Hanski et al., 2001; Shimizu et al., 2004; Arndt et al., 2008),因此,这些元素特征可对岩浆源区及演化进行示踪。本次工作中,除了 KK01-20 受蚀变影响较强外,本文测得科克辉长岩样品的主量元素(MgO, Al_2O_3, TiO_2 和 P_2O_5)、高场强元素(Th, Ti, Nb, Ta, Zr, Y 和 Hf)和稀土元素的含量变化范围很小,具有一致的原始地幔标准化曲线(表 2 和图 7),指示这些元素在后期热事件中变化较小,其特征可以用来讨论科克辉长岩岩体的岩石成因。

对于基性岩浆的研究显示,封闭的岩浆体系中在结晶过程中元素丰度虽然随之变化,而总分配系数相同或者很相近的元素比值不会因结晶作用而改变,但如有外来物质显著混染,会使得这些元素比值发生巨大变化(Cambell et al., 1993; Sun et al., 2008);总分配系数相同或者很相近、对同化混染作用敏感的元素比值,可以检验同化混染作用的指标。一般来说,随着结晶作用的进行,残余岩浆中不相容元素浓度逐渐增高(Lassiter et al., 1997),但相近元素的比值相对稳定,在地幔部分熔融过程和岩浆结晶分异过程中变化小,可以用这些不相容元素的比值来限定岩浆源区特征。Lassiter et al.(1997)指出,仅发生分离结晶作用使得岩浆岩 La/Sm 比值一般小于 5,且基本无变化;如上升过程中混染了地壳物质,则 La/Sm 比值迅速增高,一般在 5 以上。本文测试数据显示,本次测得科克辉长岩的 La/Sm 比值范围在 2.56~4.10,均小于 5,指示形成科克辉长岩的基性岩浆在上升过程中未受到显著的同化混染。科克辉长岩较小的 Nb/Ta(18.07~22.93)、Zr/Hf(31.55~34.06)、La/Yb(4.51~9.03)比值变化范围,指示了岩浆侵位过程中未发生明显的同化混染作用。另一方面,科克辉长岩的 Eu 异常不明显(δEu=0.90~1.20),表明斜长石的分离结晶作用不明显。哈克图解也显示,随着 MgO 减小,科

克辉长岩的主量元素比值没有明显的变化趋势,也指示该岩体结晶分异程度较弱。

前人研究显示,源于上、下地幔边界(White et al., 1989, 1995)或核-幔边界(Campbell et al., 1990; Campbell, 2001)的深源岩浆具有低 La/Ta(一般<15)比值,而源于岩石圈地幔(CLM)或受其混染后岩浆的 La/Ta 比值一般在 25 以上,科克辉长岩的 La/Ta 比值范围在 83.46～122.50 之间,均值 101.09,远大于 25,指示科克辉长岩源于岩石圈地幔。科克辉长岩球粒陨石标准化的$(Gd/Yb)_N$变化范围在 1.12～1.61 之间,均值为 1.31,总体具有>1.20 的特点(图 8a),指示了岩浆源区为重稀土元素发生了明显的分异作用的石榴子石源区特点(Henderson, 1984; McKenzie et al., 1991),指示其源区深度大于 75km(Hirschmann et al., 1996; Said et al., 2009)。此外,在 La/Sm-La 判别图解(图 8b)上,科克玄武岩样品在随着 La 含量增加,La/Sm 比值略有上升,但变化不大,处于分离结晶方向,指示分离结晶作用是控制该基性岩浆产生的主要方式(Cocherine, 1986)。

已有研究表明,典型的 Nb、Ta、Ti 亏损是岛弧构造环境岩浆岩的重要标志(Ionov et al., 1995; Zhao Zhenhua et al., 2006; Yuan Feng et al., 2010)。在主动大陆边缘环境中,由于大洋岩石圈的俯冲,俯冲板片会由于脱水作用而使得 Th 和 LREE 等易于迁移的元素大量进入到俯冲板片上方的地幔楔中(Saunders et al., 1996),而俯冲板片的 Nb 含量在脱水作用中很难发生迁移,会随着俯冲板块进入地幔深部演化(Gaetani et al., 1993; Pearce et al., 1995)。这一过程不仅导致了岛弧环境中地幔楔的组成及其产生的岩浆具有正 Th 和 LREE 异常、和负的 Nb 异常特点(Taylor et al., 1985; Rudnick et al., 2004),而且也使得残存的俯冲板块及其物质循环作用产生的洋岛玄武岩(OIB)和大洋高原玄武岩(OPB)具有正 Nb 异常的特点(Saunders et al., 1996; Lassiter et al., 1997)。这些岩浆作用被认为是俯冲大洋板片的物质循环(Sun et al., 1989; Brandon et al., 1993; Mahoney et al., 1995; Lassiter et al., 1997; Kerrich, et al., 1999; Rudnick et al., 2004; Said et al., 2010)。科克辉长岩除了 KK01-20 样品的 Nb/Th 比值(4.31)较高外,其他样品的 Nb/Th 比值在 1.42～2.58 之间,均值 1.79;远远小于原始地幔的 Nb/Th 比值(Nb/Th≈8, Sun et al., 1989),具有明显富集 LREE、亏损 Nb、Ta 等元素特征(图 7),指示其岩浆源区存在俯冲地壳物质混染与交代(Rudnick et al., 2003)。另外科克辉长岩具有富含磁铁矿的特征,指示了其岩浆源区为氧化的俯冲交代地幔源区。

4.3　成岩背景

前人对阿尔泰地区在石炭纪基本奠定了现今的构造格局已有共识(He Guoqi et al., 1994; Wang Jingfei et al., 2008; Tong Ying et al., 2010)。但石炭纪以来对于该区的构造演化还存在不同观点:Liu Fei et al. (2013)推断在 290～245Ma 之间,伊犁-准噶尔板块沿天山和额尔齐斯断裂带向东楔入

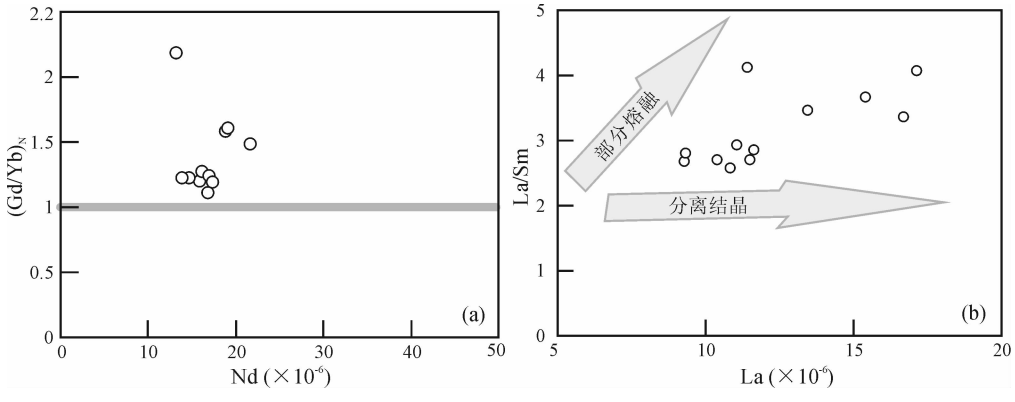

图 8　阿尔泰科克地区辉长岩的岩浆源区性质判别图解

Fig. 8　REE variations of the Keke gabbro intrusion

(a)—球粒陨石标准化 $(Gd/Yb)_N$-Nd 图解 (after Said et al., 2009; 球粒陨石数据来自 Sun et al., 1989);

(b)—La/Sm-La 图解(after Cocherine, 1986)

(a)—Chondrite-normalized $(Gd/Yb)_N$-Nd diagrams (after Said et al., 2009; the data are normalized to chondrite values of Sun et al., 1989);

(b)—La/Sm-La diagrams (after Cocherine, 1986)

到塔里木和西伯利亚两大地块之间,该区处于增生造山环境(Xiao Wenjiao et al., 2006)。Wang Tao et al.(2010)认为阿尔泰造山带石炭纪之后造山作用接近尾声,逐渐进入了造山后伸展构造背景(Deng yufeng et al., 2011, 2014)。Zou Tianren et al.(1988)认为阿尔泰地区二叠纪处于非造山环境。Pirajno (2010)对新疆地区二叠纪基性岩研究后认为,该区岩浆岩与地幔柱相关;Tong Ying et al.(2006)对阿尔泰石炭纪—二叠纪花岗岩构造背景研究显示,这些花岗岩都集中在额尔齐斯断裂带内(Sun Guihua et al., 2009),应与该断裂带在早二叠世走滑有关(Briggs et al., 2007)。

本文对科克辉长岩的地质特征研究显示,科克辉长岩侵位于泥盆纪地层中,该辉长岩与喀拉通克基性杂岩体均位于额尔齐斯断裂带南侧,年代学工作表明科克辉长岩体与喀拉通克等基性岩体均形成于早二叠世,具有相似的地球化学特征(图 7a,b),是锡泊渡、喀拉通克经哈腊苏到克孜勒他乌二叠纪镁铁质岩带的组成部分。科克辉长岩体的岩石成因显示,该基性岩浆源于氧化的俯冲交代岩石圈地幔。稀土元素显示科克辉长岩具有明显的重稀土元素分异作用($(Gd/Yb)_N>1.20$)且具有相对较高的钛浓度,与形成于大陆裂谷环境的溢流玄武岩(CFB)性质一致(Arndt et al., 2008; Lassiter et al., 1997; Lu Meihua et al., 1997; Tang Yanjie et al., 2006),如西伯利亚和德干等地的大陆溢流玄武岩(Saunders et al., 1992, 2005; Keays et al., 2007, 2010),而与攀枝花辉长岩明显不同(图 7a,b)。在

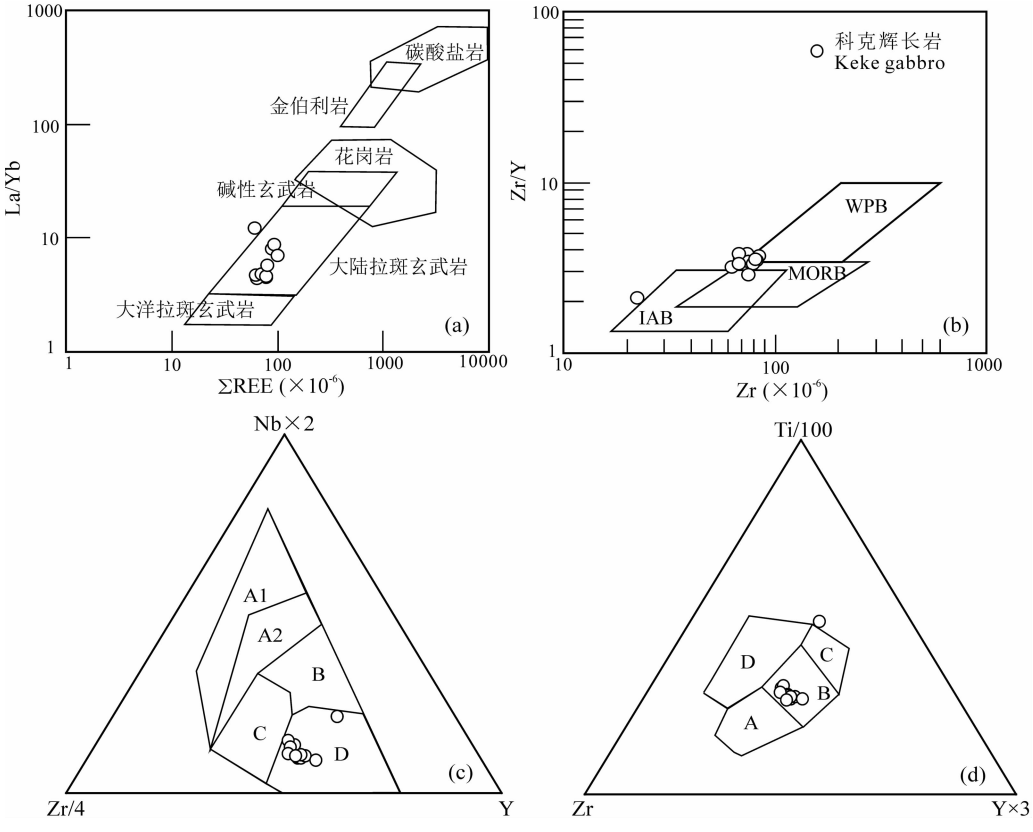

图 9 阿尔泰科克地区辉长岩的构造环境地球化学判别图解

Fig. 9 Geotectonic discrimination diagrams for the Keke mafic intrusion

(a)—∑REE-La/Yb 环境判别图解(Bartley, 1986);(b)— Zr-Zr/Y 判别图解 (Pearce et al., 1979)(WPB—板内玄武岩;IAB—岛弧玄武岩;MORB—洋中脊玄武岩);(c)— Nb×2-Zr/4-Y 三角图解 (after Meschede, 1986)(A1—板内碱性玄武岩;A2—板内玄武岩;B—富集洋中脊玄武岩;C—板内玄武岩或火山弧玄武岩 (VAB);D—正常洋中脊或火山弧玄武岩); (d)—Ti/100-Zr-Y×3 三角图解(after Pearce et al., 1973)(A—大陆弧玄武岩; B—大洋溢流玄武岩; C—低钾拉斑玄武岩; D—板内玄武岩)

(a)—∑REE-La/Yb tectonic discrimination diagram (Bartley, 1986); (b)—Zr-Zr/Y tectonic discrimination diagram (Pearce et al., 1979)(WPB—within plate basalt;IAB—island arc basalt;MORB—mid-ocean ridge basalt);(c)—Nb×2-Zr/4 -Y diagram (after Meschede, 1986)(A1—within plate alkaline basalt;A2—within plate alkaline basalt or within plate tholeiite basalt;B—enriched MORB;C—within plate basalt and volcanic arc basalt (VAB); D—normal MORB or VAB); (d)—Ti/100-Zr-Y×3 diagram (after Pearce et al., 1973)(A—continental arc basalt (CAB); B—ocean flood basalt (OFB); C—low-K tholeiitic basalt (LKT);D—WPB)

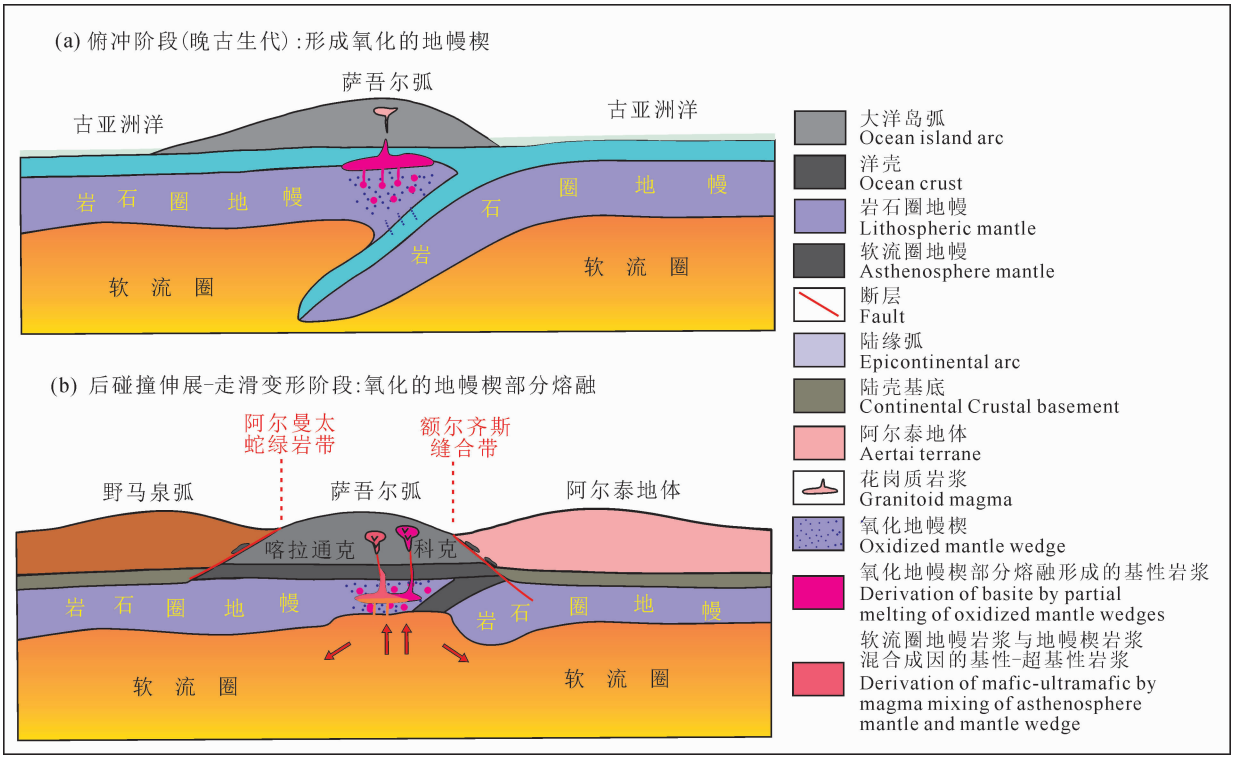

图 10　科克岩浆岩的成岩模式图

Fig. 10　The petrogenesis evolution model of the Keke gabbro intrusion in Qinghe County

∑REE-La/Yb 构造环境判别图解(图 9a)中,科克辉长岩样品除一个样品(KK01-20)外,其他均落于大陆拉斑玄武岩区域,指示形成于拉张的陆内环境;在 Zr-Zr/Y 判别图解(图 9b)上也投点于板内玄武岩与洋中脊玄武岩过渡区域,指示岩浆岩侵位于拉张构造背景。这一认识得到了在 Nb×2-Zr/4-Y(图 9c)和 T/100-Zr-Y×3 构造判别图解(图 9d)的支持。此外,科克玄武岩具有较高的 Zr/Y 比值(2.14～3.91)及较低的 Nb/Y 比值(0.09～0.21),指示为非地幔柱岩浆作用的产物(Condie,2005)。结合该区在晚古生代构造演化特点(Wang Jingbin et al., 2006),侵位于可可托海-二台断裂的西侧的早二叠世科克辉长岩很可能形成于后碰撞伸展环境,其形成均与软流圈岩浆上涌并导致被交代的地幔楔的部分熔融与岩浆混合有关,结合科克岩浆岩紧邻额尔齐斯深大断南侧分布的地质特征,其侵位可能与额尔齐斯断裂走滑作用有关。

综合以上研究,科克岩体的成岩地球动力学过程可描述如下:在晚古生代(>310Ma)科克地区处于阿尔泰南缘的增生造山作用的俯冲岛弧环境,形成的萨吾尔岛弧在形成岛弧火山岩的同时,在地幔楔位置发生弧岩浆底侵,形成逐步氧化的加厚岩石圈(图 10a)。在早二叠世(～290Ma),该区进入后碰撞伸展环境,早期加厚的岩石圈地幔发生拆沉,氧化的基性—超基性岩浆沿着深大断裂上升侵位,形成了包括科克、喀拉通克等岩体在内的额尔齐斯-玛因鄂博构造带二叠纪镁铁质—超镁铁质侵入体(图 10b)。其中,科克岩体与喀拉通克基性杂岩体相比,科克辉长岩具更明显与强烈的 Nb 与 Ta 亏损(图 7b),这可能指示科克辉长岩浆保留了更多的地幔楔的信息,而喀拉通克基性岩浆中则有较多的软流圈地幔岩浆的加入(Song and Li, 2009; Li Chusi et al., 2012; Deng Yufeng et al., 2015),这可能是铜镍矿成矿的原因与基础(Gao jianfeng and Zhou Meifu, 2013)。

5　结论

(1)科克辉长岩体形成于 291Ma 左右,属早二叠世,与北疆地区广泛发育的二叠纪铜镍矿化基性岩的侵入年龄相对应。

(2)科克辉长岩具富集大离子亲石元素和亏损高场强元素 Nb、Ta 与 Ti 的特征,可能起源于氧化的俯冲交代地幔楔的部分熔融,岩浆在上升演化过程中受地壳物质混染作用较弱。

(3)科克辉长岩与喀拉通克基性杂岩体的形成均与软流圈岩浆上涌、并导致被交代的地幔楔的部

分熔融与岩浆混合有关,岩体侵位受额尔齐斯走滑断裂控制。

致谢:本文的研究工作得到了新疆"305"项目办公室、新疆有色706地质队和中国科学院地质与地球物理研究所的大力支持;论文得到了秦克章研究员的指导和支持;成文过程中与合肥工业大学张达玉博士进行有益讨论,在此一并致以诚挚的感谢!

References

Arndt N, Lesher C M, Barnes S J. 2008. Komatiite. Cambridge University Press, 1~488.

Barley M E, Kerrich R, Reudavy I, Xie Q. 2000. Late Archean Ti-rich, Al-depleted komatiites and komatiitic volcaniclastic rocks from the Murchison Terrane in western Australia. Australian Journal of Earth Sciencess, 47(5): 873~883.

Bartley J M. 1986. Evaluation of REE mobility in low grade metabasalt using mass-balance calculations. Norsk Geo Tidssk, 66(2): 145~152.

Brandon A D, Hooper P R, Goles G G, Lamber R S J. 1993. Evaluating crustal contamination in continental basalts: the isotopic composition of the Picture Gorge Basalt of the Columbia River Basalt Group. Contributions to Mineralogy and Petrology, 114(4): 452~464.

Briggs S M, Yin A, Manning C E, Chen Z L, Wang X F, Grove L. 2007. Late Paleozoic tectonic history of the Ertix fault in the Chinese Altai and its implications for the development of the Central Asian Orogenic System. Geological Society of America Bulletin, 119(7~8): 944~960.

Cai Keda, Sun Min, Jahn B, Xiao Wenjiao, Long Xiaoping, Chen Huayong, Xia Xiaoping, Chen Ming, Wang Xiangsong. 2016. Petrogenesis of the Permian intermediate-mafic dikes in the Chinese Altai, Northwest China: Implication for a postaccretion extensional scenario. Journal of Geology, 124(4): 481~500.

Campbell I H, Griffiths R W. 1990. Implications of mantle plume structure for the evolution of flood basalts. Earth and Planetary Science Letters, 99(1): 79~93.

Campbell I H, Griffiths R W. 1993. The evolution of the mantle's chemical structure. Lithos, 30(3~4): 389~399.

Campbell I H. 2001. Identification of ancient mantle plumes. Special Paper of the Geological Society of America, 352: 5~21.

Chen Shiping, Wang Denghong, Qu Wenjun, Chen Zhenghui, Gao Xiaoli. 2005. Geologicalfeatures and ore formation of the Hulu Cu-Ni sulfide deposit, eastern Tianshan, Xinjiang. Xinjiang Geology, 23(3): 230~233 (in Chinese with English abstract).

Cocherine A. 1986. Systematic use of trace element distribution patterns in log-log diagram for plutonic suites. Geochimica et Cosmochimica Acta, 50(11): 2517~2522.

Condie K C. 2005. High field strength element ratios in Archean basalts: a window to evolving sources of mantle plumes? Lithos, 79(3): 491~504.

Deng Yufeng, Song Xieyan, Jie Wei, Cheng Songlin, Li Jun. 2011. Petrogensis of the Huangshandong Ni-Cusulfide-bearing mafic-ultramafic intrusion, northern Tianshan, Xinjiang: Evidence from major and trace elements and Sr-Nd isotope. Acta Geologica Sinica, 85(9): 1435~1451 (in Chinese with English abstract).

Deng Y F, Song X Y, Chen L M, Zhou T F, Pirajno F, Yuan F, Xie W, Zhang D Y. 2014. Geochemistry of the Huangshandong Ni-Cu deposit in northwestern China: implications for the formation of magmatic sulfide mineralization in orogenic belts. Ore Geology Reviews, 56: 181~198.

Deng Y F, Song X Y, Hollings P, et al. 2015. Role of asthenosphere and lithosphere in the genesis of the Early Permian Huangshan mafic-ultramafic intrusion in the Northern Tianshan, NW China. Lithos, 227: 241~254.

Dong Y, Ge W C, Yang H, Xu W L, Bi J H, Wang Z H. 2017. Geochemistry and geochronology of the Late Permian mafic intrusions along the boundary area of Jiamusi and Songnen-Zhangguangcai Range massifs and adjacent regions, northeastern China: Petrogenesis and implications for the tectonic evolution of the Mudanjiang Ocean. Tectonophysics, 694: 356~367.

Ewart A. 1982. The mineralogy and petrology of Tertiary-Recent orogenic volcanic rocks with special reference to the andesitic-basaltic compositional range. Orogenic Andesites and Related Rocks, 25~95.

Fu Chao, Liang Guanghe, Xu Xingwang, Cheng Songlin, Li Jun. 2010. Magnetotelluric study on the Kalaxianger fault zone in the north margin of Junggar, Xinjiang, China. Acta Petrologica Sinica, 26(10): 3007~3016 (in Chinese with English abstract).

Gaetani G A, Grove T L, Bryan W B. 1993. The influence of water on the petrogenesis of subduction-related igneous rocks. Nature, 365(6444): 332~334.

Gao J F, Zhou M F, Lightfoot P C, Wang C Y, Qi L. 2012. Origin of PGE-poor and Cu-rich magmatic sulfides from the Kalatongke deposit, Xinjiang, Northwest China. Economic Geology, 107(3): 481~506.

Gao J F, Zhou M F. 2013. Generation and evolution of siliceous high magnesium basaltic magmas in the formation of the Permian Huangshandong intrusion (Xinjiang, NW China). Lithos, 162~163(2): 128~139.

Gu Lianxing, Zhang Zunzhong, Wu Changzhi, Wang Yinxi, Tang Junhua, Wang Chuansheng, Xi Aihua, Zheng Yuanchuan. 2006. Some problems on granites and vertical growth of the continental crust in the eastern Tianshan Mountains, NW China. Acta Petrologica Sinica, 22(5): 1103~1120 (in Chinese with English abstract).

Han Baofu, Ji Jianqing, Song Biao, Chen Lihui, Li Zonghuai. 2004. SHRIMP zircon U-Pb ages of Kalatongke No. 1 and Huangshandong Cu-Ni-bearing mafic-ultramafic complexes, North Xinjiang, and geological implications. Chinese Science Bulletin, 49(22): 2424~2429.

Han Chunming, Xiao Wenjiao, Zhao Guochun, Qu Wenjun, Mao Qigui, Du Andao. 2006. Re-Os isotopic analysis of the Kalatongke Cu-Ni Sulfile deposit, northern Xinjiang, NW China, and its geological implication. Acta Petrologica Sinica, 22(1): 163~170 (in Chinese with English abstract).

Hanski E, Huhma H, Rastas P, Kamenetsky V S. 2001. The Palaeoproterozoic komatiite-picrite association of Finnish Lapland. Journal of Petrology, 42(5): 855~876.

He Guoqi, Li Maoong, Liu Dequan. 1994. The crustal evolution and mineralization in north Xinjiang, China. Wulumuqi: People's Publishing House in Xinjiang, 1~437 (in Chinese).

Henderson P, Wood R J. 1984. Reaction relationship of chrome-spinel in igneous rocks-further evidence from the layered intrusions of Rhum and Mull, Inner Hebrides, Scotland. Contributions to Mineralogy and Petrology, 78(3): 225~229.

Hirschmann M M, Stolper E M. 1996. A possible role for garnet pyroxenite in the origin of the garnet signature in MORB. Contributions to Mineralogy and Petrology, 124(2): 185~208.

Hu Xiaoqing, Xi Aihua, Xiang Lei, Xie Guanzhi, Xiao Siyu, Sun Hongru, Shi Guipeng. 2016. Geochemical characteristics of ore-bearing gabbro from Panzhihua, Sichuan Province, and its metallogenic significance. Global Geology, 35(2): 395~402 (in Chinese with English abstract).

Ionov D A, Hofmann A W. 1995. Nb/Ta-rich mantle amphiboles and micas: Implications for subduction-related metasomatic trace element fractionations. Earth and Planetary Science Letters, 131(3): 341~356.

Jiang Changyi, Cheng Songlin, Ye Shufeng, Xia Mingzhe, Jiang Hanbing, Dai Yucai. 2006. Lithogeochemistry and petrogenesis of Zhongposhanbei mafic rock body, at Beishan region, Xinjiang. Acta Petrolohica Sinica, 22(1): 115～126 (in Chinese with English abstract).

Jiang Changyi, Xia Mingzhe, Qian Zhuangzhi, Yu Xu, Lu Ronghui, Guo Fangfang. 2009. Petrogenesis of Kalatongke mafic rock intrusions, Xinjiang. Acta Petrolohica Sinica, 25(4): 749～764 (in Chinese with English abstract).

Jiao Jiangang, Wang Yong, Qian Zhuangzhi, Wang Bin, Lu Hao, Liu Huan, Zheng Pengpeng. 2014. Tentative discussion on rock-forming and ore-forming mechanism of Kalatongke Cu-Ni sulfide deposit and chronology of Kalatongke Y9 intrusion. Mineral Deposits, 33(4): 675～688 (in Chinese with English abstract).

Keays R R, Lightfoot P C. 2007. Siderophile and chalcophile metal variations in Tertiary picrites and basalts from West Greenland with implications for the sulphide saturation history of continental flood basalt magmas. Mineralium Deposita, 42(4): 319～336.

Keays R R, Lightfoot P C. 2010. Crustal sulfur is required to form magmatic Ni-Cu sulfide deposits: evidence from chalcophile element signatures of Siberian and Deccan Trap basalts. Mineralium Deposita, 45(3): 241～257.

Kerrich R, Polat A, Wyman D, Hollings P. 1999. Trace element systematics of Mg-, to Fe-tholeiitic basalt suites of the Superior Province: implications for Archean mantle reservoirs and greenstone belt genesis. Lithos, 46(1): 163～187.

Lassiter J C, DePaolo D J. 1997. Plumes/lithosphere interaction in the generation of continental and oceanic flood basalts: Chemical and isotope constraints. American Geophysical Union, 100: 335～355.

Li C S, Thakurta J, Ripley E M. 2012. Low-Ca contents and kink-banded textures are not unique to mantle olivine: evidence from the Duke Island complex, Alaska. Mineralogy and Petrology, 104: 147～153.

Li Huaqin, Mei Yuping, Qu Wenjun, Cai Hong, Du Guomin. 2009. SHRIMP zircon U-Pb and Re-Os dating of No. 10 intrusive body and associated ores in Pobei mafic-ultramafic belt of Xinjiang and its significance. Mineral Deposits, 28(5): 633～642 (in Chinese with English abstract).

Li Huaqin, Xie Caifu, Chang Hailiang. 1998. The geochronology of the nonferrous metal the ore deposits in north Xinjiang. Beijing: Geological Publishing House, 1～264 (in Chinese).

Li Xianhua, Liu Ying, Tu Xianglin, Hu Guangqian, Zeng Wen. 2002. Precise determination of chemical compositions in silicate rocks using ICP-AES and ICP-MS: A comparative study of sample digestion techniques of slkali fusion and acid dissolution. Geochimica, 31(3): 289～294 (in Chinese with English abstract).

Li Xianhua, Liu Yu, Li Qiuli, Guo Chunhua, Chamberlain K R. 2009. Precise determination of Phanerozoic zircon Pb/Pb age by multi-collector SIMS without external standardization. Geochemistry Geophysics Geosystems, 10(4): 1～21.

Li Yuechen, Zhao Guochun, Qu Wenjun, Pan Chengze, Mao Qigui, Du Andao. 2006. Re-Os isotopic dataing of the Xinjiang deposit, East Tianshan, NW China. Acta Petrolohica Sinica, 22(1): 245～251 (in Chinese with English abstract).

Liu Fei, Wang Zhenyuan, Lin Wei, Chen Ke, Jiang Lin, Wang Qingchen. 2013. Structure defodmation and tectonic significance of Erqis fault zone in the southern margin of Chinese Altay. Acta Petrolohica Sinica., 29(5): 1811～1824 (in Chinese with English abstract).

Lu Meihua, Hofmann A W, Mazzucchelli M, Rivalenti G. 1997. The mafic-ultramafic complex near Finero (Ivrea-Verbano Zone), I. chemistry of MORB-like magmas. Chemical Geology, 140(3～4): 207～222.

Mahoney J J, Jones W B, Frey F A, Salters V J M, Pyle D G, Davies H L. 1995. Geochemical characteristics of lavas from Broken Ridge, the Naturaliste Plateau and southernmost Kerguelen Plateau: Cretaceous plateau volcanism in the southeast Indian Ocean. Chemical Geology, 120(3～4): 315～345.

Mao Jingwen, Yang Jianmin, Han Chunming, Wang Zhiliang. 2002. Metallogenic systems of polymetallic copper and gold deposits and related metallogenic geodynamic model in eastern Tianshan, Xinjiang. Earth Science-Journal of China University of Geosciences, 27(4): 413～424 (in Chinese with English abstract).

Mao Jingwen, Pirajno F, Zhang Zuoheng, Chai Fengmei, Wu Hua, Chen Shiping, Cheng Linsong, Yang Jianmin, Zhang Changqing. 2008. A review of the Cu-Ni sulphide deposits in the Chinese Tianshan and Altay orogens (Xinjiang Autonomous Region, NW China): Principal characteristics and ore-forming processes. Journal of Asian Earth Sciences, 32(2～4): 184～203.

Mao Qigui. 2008. Paleozoic to Early Mesozoic accretionary and collisional tectonics of the Beishan and adjacent area, northwest China. Doctor degress thesis of Institute of Geology and Geophysics, Chinese Academy of Sciences, 1～227 (in Chinese with English abstract).

Mckenzie D, O'Nions K. 1991. Partial melt distributions from inversion of rare earth element concentrations. Journal of Petrology, 32(6): 1021～1091.

Meschede M. 1986. A method of discriminating between different types of mid-ocean ridge basalts and continental tholeiites with the Nb-Zr-Y diagram. Chemical Geology, 56(3): 207～218.

Middlemost E A K. 1994. Naming materials in the magma/igneous rock system. Earth Science Reviews, 37(3): 215～224.

Pearce J A, Cann J R. 1973. Tectonic setting of basic volcanic rocks determined using trace element analyses. Earth and Planetary Science Letters, 19(2): 290～300.

Pearce J A, Norry M J. 1979. Petrogenetic implications of Ti, Zr, Y and Nb variations in volcanic rocks. Contrib. Mineral. Petrol., 69(1): 33～47.

Pearce J A, Peate D W. 1995. Tectonic implications of the composition of volcanic arc lavas. Annual Review of Earth and Planetary Sciences, 23: 251～285.

Pirajno F. 2010. Intracontinental strike-slip faults, associated magmatism, mineral systems andmantle dynamics: examples from NW china and Altay-Sayan (Siberia). Journal of Geodynamics, 50(3～4): 325～346.

Qin K Z, Sun Shu, Li Jiliang, Fang Tonghui, Wang Shulai, Liu Wei. 2002. Paleozoic epithermal Au and porphyry Cu deposits in North Xinjiang, China: epochs, features, tectonic linkage and exploration significance. Resource Geology, 52(4): 291～300.

Qin Kezhang. 2000. Metellogenses inrelation to Central-Asia style orogeny of northern Xinjiang. Post-Doctor research report. Beijing: Institute of Geology and Geophysics, Chinese Academy of Sciences, 1～194 (in Chinese with English abstract).

Qin Kezhang, Tang Dongmei, Su Benxun, Mao Yajing, Xue Shengchao, Tian Ye, Sun He, San Zhujin, Xiao Qinghua, Deng Gang. 2012. The tectonic setting, style, basic feature, relative erosion Deee, ore-bearing evaluation sign, potential analysis of mineralization of Cu-Ni-bearing Permian mafic-ultramafic complexes, northern Xinjiang. Northwestern Geology, 45(4): 83～116 (in Chinese with English abstract).

Qin K Z, Sun B X, Sakyi P A, Tang D M, Li X H, Sun H, Xiao Q H, Liu P P. 2011. SIMS zircon U-Pb geochronology and Sr-Nd isotopes of Ni-Cu-bearing mafic-ultrafic in-trusions in eastern Tianshan and Beishan in correlation with flood basalts in Tarim basin (NW China): constraints on a ca. 280 Ma mantle plume. American Journal of Science, 311 (3): 237～260.

Rudnick R L, Gao Shan, Ling Wenli, Liu Yongshen, McDonough W F. 2004. Petrology and geochemistry of spinel peridotite xenoliths from Hannuoba and Qixia, North China craton. Lithos, 77(1～4): 609～637.

Rudnick R L, Gao Shan. 2003. Composition of the continental crust. In: Rudnick R L, ed. The Crust. Vol. 3 of Holland H D, Turekian K K, eds. Treatise on Geochemistry. Oxford: Elsevier-Pergamon, 1～64.

Said N, Kerrich R. 2009. Geochemistry of coexisting depleted and enriched Paringa basalts, in the 2.7 Ga Kalgoorlie terrane, Yilgarn craton, western Australia: Evidence for a heterogeneous mantle plume event. Precambrian Research, 174(3): 287～309.

Said N, Kerrich R. 2010. Elemental and Nd-isotope systematics of the Upper Basalt Unit, 2.7 Ga Kambalda Sequence: Quantitative modeling of progressive crustal contamination of plume asthenosphere. Chemical Geology, 273(3): 193～211.

Saunders A D, England R W, Reichow M K, White R V. 2005. A mantle plume origin for the Siberian traps: uplift and extension in the West Siberian basin, Russia. Lithos, 79(3): 407～424.

Saunders A D, Storey M, Kent R W, Norry M J. 1992. Consequences of plume-lithosphere interactions. Geological Society of London Special Publications, 68(1): 41～60.

Saunders A D, Tarney J, Kerr A C, Kent R W. 1996. The formation and fate of Large Igneous Provinces. Lithos, 37(2～3): 81～95.

Sengör A M C, Natal'in B A, Burtman V S. 1993. Evolution of the Altaid tectonic collage and Paleozoic crustal growth in Asia. Nature, 364: 299～307.

Shimizu K, Nakamura E, Maruyama S, Kabayashi K. 2004. Discovery of Archean continental and mantle fragments inferred from xenocrysts in komatiites, the Belingwe greenstone belts, Zimbabwe. Geology, 32(4): 285～288.

Song X Y, Li X R. 2009. Geochemistry of the Kalatongke Ni-Cu-(PGE) sulfide deposit, NW China: implications for the formation of magmatic sulfide mineralization in a postcollisional environment. Mineralium Deposita, 44(3): 303～327.

Sun Guihua, Li Jintie, Yang Tiannan, Li Yaping, Zhu Zhixin, Yang Zhiqing. 2009. Zircon SHRIMP U-Pb dating of two linear granite plutons in southern Altay Mountains and its tectonic implications. Geology China, 26(5): 976～987 (in Chinese with English abstract).

Sun S S, McDonough W F. 1989. Chemical and isotopic systematic of oceanic basalts: implications for mantle composition and processes. Geological Society Special Publication, 42(1): 313～345.

Sun Weidong, Hu Yanhua, Kamenetsky V S, Eggins S M, Chen M, Arculus R J. 2008. Constancy of Nb/U in the mantle revisited. Geochimica et Cosmochimica Acta, 72(14): 3542～3549.

Tang Yanjie, Zhang Hongfu, Ying Jifeng. 2006. Asthenosphere-lithospheric mantle interaction in an extensional regime: implication from the geochemistry of Cenozoic basalts from Taihang Mountains, North China Craton. Chemical Geology, 233(2～3): 309～327.

Taylor S R, McLennan S M. 1985. The Continental Crust: Its Composition and Evolution: An Examination of the Geochemical Record Preserved in Sedimentary Rocks. Oxford: Blackwell Scientific, 1～312.

Tang Dongmei, Qin Kezhang, Sun He, Sun Benxun, Xiao Qinghua, Cheng Songlin, Li Jun. 2009. Lithological, chronological and geochemical chareacteristics of Tianyu Cu-Ni deposit: Constraints on source and genesis of mafic-ultramafic intrusions in eastern Xinjiang. Acta Petrologica Sinica, 25(4): 817～831 (in Chinese with English abstract).

Tong Ying, Hong Dawei, Wang Tao, Wang Shiguang, Han Baofu. 2006. Times U-Pb zircon ages of Fuyun post-orogenic linear granite plutons on the southern margin of Altay orogenic belt and their implications. Acta Petrologicaet Minerlogica, 25(2): 85～89 (in Chinese with English abstract).

Tong Ying, Hong Dawei, Wang Tao, Shi Xingjun, Zhang Jianjun, Zeng Tao. 2010. Spatial and temporal distribution of granitoids in the middle segment of the Sino-Mongolian border and its tectonic and metallogenic implications. Diqiu Xuebao (Acta Geoscientica Sinica), 31(3): 395～412 (in Chinese with English abstract).

Wang Hong, Qu Wenjun, Li Huaqin, Chen Shiping. 2007. Dating anddiscussion on the rock forming and ore forming age of newly discovered Cu-Ni sulfide deposits in Hami, Xinjiang. Acta Geologica Sinica, 81(4): 526～530 (in Chinese with English abstract).

Wang Jingbin, Wang Yuwang, Zhou Taofa. 2008. Metallogenic spectrum related to post-collisional mantle-derived magma in north Xinjiang. Acta Petrologica Sinica, 24(4): 743～752 (in Chinese with English abstract).

Wang Jingbin, Xu Xin. 2006. Post-collissionaltectonic evolution and metallogenesis in northern Xinjiang, China. Acta Geologica Sinica, 80(1): 23～31 (in Chinese with English abstract).

Wang Runmin, Li Sichu. 1987. Physicochemical condition of rock formation and mineralization of Huangshandong magmatogenic sulfide deposit Hami, Xinjiang, China. Journal of Chengdu College of Geology, 14(3): 1～9 (in Chinese with English abstract).

Wang Tao, Tong Ying, Li Shan, Zhang Jianjun, Shi Xingjun, Li Jintie, Han Baofu, Hong Dawei. 2010. Spatial and temporal variations of granitoids in the Altay oroogen and their implications for tectonic setting and crustal growth: perspectives from Chinese Altay. Acta Petrologica et Mineralogica, 29(6): 595～618 (in Chinese with English abstract).

Wang Yuwang, Wang Jingbin, Wang Lijuan, Fang Tonghui. 2007. Magma-mixing genesis of quartz monzodioirte in the Weiya, Xinjiang. Acta Petrologica Sinica, 23(4): 733～746 (in Chinese with English abstract).

White R S, McKenzie D P. 1989. Magmatism at rift zones: the generation of volcanic contonental margins and flood basalts. Journal of Geophysical Research Solid Earth, 94(B6): 7685～7729.

White R S, Mckenzie D P. 1995. Mantle plume and flood basalt. Journal of Geophysical Research Solid Earth, 100(B9): 17543～17585.

Winchester J A, Floyd P A. 1976. Geochemical magma type discrimination: application to altered and metamorphosed basic igneous rocks. Earth and Planetary Science Letters, 28(3): 459～469.

Windley B F, Kröner A, Guo Jinghui, Qu Guosheng, Li Yingyi, Zhang Chi. 2002. Neoproterozoic to Paleozoic geology of the Altai orogen, NW China: new zircon age data and tectonic evolution. The Journal of Geology, 110(6): 719～737.

Wu Hua, Li Huaqin, Mo Xinhua, Chen Fuwen, Lu Yuanfa, Mei Yuping, Deng Gang. 2005. Age of the Baishiqun mafic-ultramafic complex, Hami, Xinjiang and its geolohical significance. Acta Geologica Sinica, 79(4): 498～502 (in Chinese with English abstract).

Xue Chunji, Zhao Zhanfeng, Wu Gangguo, Dong Lianhui, Feng Jing, Zhang Zhaochong, Zhou Gang, Chi Guoxiang, Gao Jinggang. 2010. The multiperiodic superimposed porphyry copper mineralization in central Asian Tectonic Region: A case study of geology, geochemistry and chronology of Halasu copper deposit, Southeastern Altai, China. Earth Frontiers, 17(2): 53～82 (in Chinese with English abstract).

Xiao Wenjiao, Han Chunming, Yuan Chao, Chen Hanlin, Sun Min, Lin Shoufa, Li Zilong, Mao Qigui, Zhang Jien, Sun Shu, Li Jiliang. 2006. UniqueCarboniferous-Permian tectonic-metallogenic framework of northern Xinjiang (NW China): constraints for the tectonics of the southern paleoasian domain. Acta Petrologica Sinica, 22(5): 1062～1076 (in Chinese with English abstract).

Xiao Wenjiao, Windley B F, Hao J, Zhai M G. 2003. Accretion leading to collision and the Permian Solonker suture, Inner Mongolia, China: termination of the central Asian orogenic belt. Tectonics, 22(6): 1069.

Xu Xingwang, Qin Kezhang, San Jinzhu, Wang Yu, Hui Weidong, Kang Feng, Mao Qian, Li Jinxiang, Sun He, Ma Yuguang. 2006. Discovery of layered mafic-ultramafic intrusives formed in 545Ma in the Sidingheishan area, eastern Tianshan, China and its significances for tectonics and Cu-Ni mineralization. Acta Petrologica Sinica, 22(11): 2665～2676 (in Chinese with English abstract).

Xue Shengchao, Qin K Z, Li Chusi, Tang Dongmei, Mao Yajing, Qi Liang, Ripley E M. 2016. Geochronological, petrological and geochemical constraints on Ni-Cu sulfide mineralization in the Poyi ultramafic-troctolitic intrusion in the northeast rim of the Tarim craton, western China. Economic Geology, 111(6): 1465～1484.

Yuan Feng, Zhou Taofa, Zhang Dayu, Fan Yu, Liu Shuai, Peng Mingxing, Zhang Jiandian. 2010. Source, evolution and tectonic setting of the basalts from the native copper mineralization area in eastern Tianshan, Xinjiang. Acta Petrologica Sinica, 26(2): 533～546 (in Chinese with English abstract).

Zhang Dayu, Zhou Taofa, Yuan Feng, Liu Shuai, Xu Chao, Ning Fuquan. 2012. Geochronlogy and geological indication of the native copper mineralized basalt formation in Jueluotage area, eastern Tianshan, Xinjiang. Acta Petrologica Sinica, 28(8): 2393～2400 (in Chinese with English abstract).

Zhang Zuoheng, Cai Fengmei, Du Andao, Zhang Zhaochong, Yan Shenghao, Yang Jianmin, Qu Wencai, Wang Zhiliang. 2005. Re-Os dating and ore-forming material tracing of the Karatungk Cu-Ni sulfide deposit in northern Xinjiang. Acta Petrologicaet Mineralogica, 24(4): 285 ～ 293 (in Chinese with English abstract).

Zhao Zhenhua, Wang Qiang, Xiong Xiaolin, Zhang Haiyang, Niu Hecai, Xu Jifeng, Bai Zhenghua, Qiao Yulou. 2006. Two types of adakites in north Xinjiang, China. Acta Petrologica Sinica, 22(5): 1249～1265 (in Chinese with English abstract).

Zhou Meifu, Lesher C M, Yang Zhengxing, Li Jianwei, Sun Min. 2004. Geochemistry and petrogenesis of 270Ma Ni-Cu-(PGE) sulfide-bearing mafic intrusions in the Huangshan district, eastern Xinjiang, Northwest China: implications for the tectonic evolution of the Central Asian orogenic belt. Chemical Geology, 209(3): 233～257.

Zhou Taofa, Yuan Feng, Zhang Dayu, Fan Yu, Liu Ming, Peng Mingxing, Zhang Jiandian. 2010. Geochronology, tectonic setting and minerlization of granitoids in Jueluotage area, eastern Tianshan, Xinjiang. Acta Petrologica Sinica, 26(2): 478～502 (in Chinese with English abstract).

Zhou Tianren, Cao Huizhi, Wu Baiqing. 1988. Orogenic and anorogenic granitoids of the altay mountains, Xinjiang and their discrimination criteria. Acta Geologica Sinica, 62(3): 228～243 (in Chinese with English abstract).

参 考 文 献

陈世平,王登红,屈文俊,郑陈辉,高晓理. 2005. 新疆葫芦铜镍硫化物矿床的地质特征与成矿时代. 新疆地质,23(3): 230～233.

邓宇峰,宋谢炎,颉炜,程松林,李军. 2011. 新疆北天山黄山东含铜镍矿镁铁-超镁铁岩体的岩石成因:主量元素、微量元素和 Sr-Nd 同位素证据. 地质学报,85(9): 1435～1451.

符超,梁光河,徐兴旺,蔡新平,武炜,李志远,杜世俊. 2010. 准噶尔北缘卡拉先格尔断裂带深部结构的 MT 探测. 岩石学报,26(10): 3007～3016.

顾连兴,张遵忠,吴昌志,王银喜,唐俊华,汪传胜,郗爱华,郑远川. 2006. 关于东天山花岗岩与陆壳垂向增生的若干认识. 岩石学报,22(5): 1103～1120.

韩宝福,季建清,宋彪,陈立辉,李宗怀. 2004. 新疆喀拉通克和黄山东含铜镍矿镁铁-超镁铁杂岩体的 SHRIMP 锆石 U-Pb 年龄及其地质意义. 科学通报,49(22): 2324～2328.

韩春明,肖文交,赵国春,屈文俊,毛启贵,杜安道. 2006. 新疆喀拉通克铜镍硫化物矿床 Re-Os 同位素研究及其地质意义. 岩石学报,22(1): 163～170.

何国琦,李茂松,刘德权等主编. 1994. 中国新疆古生代地壳演化及成矿. 乌鲁木齐:新疆人民出版社,1～437.

胡孝清,郗爱华,向雷,谢官志,肖嗣禹,孙鸿儒,石桂鹏. 2016. 四川攀枝花含矿辉长岩地球化学及成矿意义. 世界地质,35(2): 0395～402.

姜常义,程松林,叶书锋,夏明哲,姜寒冰,代玉财. 2006. 新疆北山地区中坡山北镁铁质岩体岩石地球化学与岩石成因. 岩石学报,22(1): 115～126.

姜常义,夏明哲,钱壮志,余旭,卢荣辉,郭芳放. 2009. 新疆喀拉通克镁铁质岩体群的岩石成因研究. 岩石学报,25(4): 749～764.

焦建刚,王勇,钱壮志,王斌,鲁浩,刘欢,郑鹏鹏. 2014. 新疆喀拉通克铜镍硫化物矿床 Y9 岩体年代学与成岩成矿机制探讨. 矿床地质,33(4): 675～688.

李华芹,梅玉萍,屈文俊,蔡红,杜国民. 2009. 新疆坡北基性～超基性岩带 10 号岩体 SHRIMP U-Pb 和矿石 Re-Os 同位素定年及其意义. 矿床地质,28(5): 633～642.

李华芹,谢才富,常海亮. 1998. 新疆北部有色贵金属矿床成矿作用年代学. 北京:地质出版社,1～264.

李献华,刘颖,涂湘林,胡光黔,曾文. 2002. 硅酸盐岩石化学组成的 ICP-AES 和 ICP-MS 准确测定:酸溶与碱熔分解样品方法的对比. 地球化学,31(3): 289～294.

李月臣,赵国春,屈文俊,潘成泽,毛启贵,杜安道. 2006. 新疆香山铜镍硫化物矿床的 Re-Os 同位素测定. 岩石学报,22(1): 245～251.

刘飞,王镇远,林伟,陈科,姜琳,王清晨. 2013. 中国阿尔泰造山带南缘额尔齐斯断裂带的构造变形及意义. 岩石学报,29(5): 1811～1824.

毛景文,杨建民,韩春明,王志良. 2002. 东天山铜金多金属矿床成矿系统和成矿地球动力学模型. 中国地质大学学报(地球科学),27(4): 413～424.

毛启贵. 2008. 北山及邻区古生代—早中生代增生与碰撞大地构造格局. 北京:中国科学院大学博士学位论文,1～227.

秦克章. 2000. 新疆北部中亚型造山与成矿作用. 中国科学院地质与地球物理研究所博士后研究工作报告,1～194.

秦克章,唐冬梅,苏本勋,毛亚晶,薛胜超,田野,孙赫,三金柱,肖庆华,邓刚. 2012. 北疆二叠纪镁铁-超镁铁岩铜、镍矿床的构造背景、岩体类型、基本特征、相对剥蚀程度、含矿性评价标志及成矿潜力分析. 西北地质,45(4): 83～116.

孙桂华,李锦轶,杨天南,李亚萍,朱志新,杨之青. 2009. 阿尔泰山脉南部线性花岗岩锆石 SHRIMP U-Pb 定年及其地质意义. 中国地质,36(5): 976～987.

唐冬梅,秦克章,孙赫,苏本勋,肖庆华,程松林,李军. 2009. 天宇铜镍矿床的岩相学、锆石 U-Pb 年代学、地球化学特征:对东疆镁铁-超镁铁质岩体源区和成因的制约. 岩石学报,25(4): 817～831.

童英,洪大卫,王涛,王式洸,韩宝福. 2006. 阿尔泰造山带南缘富蕴后造山线形花岗岩体锆石 U-Pb 年龄及其地质意义. 岩石矿物学杂志,25(2): 85～89.

童英,洪大卫,王涛,史兴俊,张建军,曾涛. 2010. 中蒙边境中段花岗岩时空分布特征及构造和找矿意义. 地球学报,31(3): 395～412.

王虹,屈文俊,李华芹,陈世平. 2007. 哈密地区新发现铜镍硫化物矿床成岩成矿时代的测定及讨论. 地质学报,81(4): 526～530.

王京彬,王玉往,周涛发. 2008. 新疆北部后碰撞与幔源岩浆有关的成矿谱系. 岩石学报,24(4): 743～752.

王京彬,徐新. 2006. 新疆北部后碰撞构造演化与成矿. 地质学报,80(1): 23～31.

王润民,李思楚. 1987. 新疆哈密黄山东铜镍硫化物矿床成岩成矿物理化学条件. 成都地质学院学报,14(3): 1～9.

王涛,童英,李舢,张建军,史兴俊,李锦轶,韩宝福,洪大卫. 2010. 阿尔泰造山带花岗岩时空演变、构造环境及地壳生长意义——以中国阿尔泰为例. 岩石矿物学杂志,29(6): 595～618.

王玉往,王京彬,王莉娟,方同辉. 2007. 新疆尾亚地区石英二长闪长岩的岩浆混合成因. 岩石学报,23(4):733～746.
吴华,李华芹,莫新华,陈富文,路远发,梅玉萍,邓岗. 2005. 新疆哈密白石泉铜镍矿区基性-超基性岩的形成时代及其地质意义. 地质学报,79(4):498～502.
薛春纪,赵战锋,吴淦国,董连慧,冯京,张招崇,周刚,池国祥,高景岗. 2010. 中亚构造域多期叠加斑岩铜矿化:以阿尔泰东南缘哈腊苏铜矿床地质、地球化学和成岩成矿时代研究为例. 地学前缘,17(2):53～82.
肖文交,韩春明,袁超,陈汉林,孙敏,林寿发,厉子龙,毛启贵,张继恩,孙枢,李继亮. 2006. 新疆北部石炭纪—二叠纪独特的构造-成矿作用:对古亚洲洋构造域南部大地构造演化的制约. 岩石学报,22(5):1062～1076.
徐兴旺,秦克章,三金柱,王瑜,惠卫东,康峰,毛骞,李金祥,孙赫,马玉光. 2006. 东天山四顶黑山地区 545Ma 层状镁铁质-超镁铁质岩体的发现及其大地构造学和成矿学意义. 岩石学报,22(11):2665～2676.
袁峰,周涛发,张达玉,范裕,刘帅,彭明兴,张建滇. 2010. 东天山自然铜矿化带玄武岩的起源、演化及成岩构造背景. 岩石学报,26(2):533～546.
张达玉,周涛发,袁峰,刘帅,许超,宁福泉. 2012. 新疆东天山觉罗塔格地区自然铜矿化玄武岩的成岩年代及其地质意义. 岩石学报,28(8):2392～2400.
张作衡,柴凤梅,杜安道,张招崇,闫升好,杨建民,屈文俊,王志良. 2005. 新疆喀拉通克铜镍硫化物矿床 Re-Os 同位素测年及成矿物质来源示踪. 岩石矿物学杂志,24(4):285～293.
赵振华,王强,熊小林,张海祥,牛贺才,许继峰,白正华,乔玉楼. 2006. 新疆北部的两类埃达克岩. 岩石学报,22(5):1249～1265.
周涛发,袁峰,张达玉,范裕,刘帅,彭明兴,张建滇. 2010. 新疆东天山觉罗塔格地区花岗岩类年代学、构造背景及其成矿作用研究. 岩石学报,26(2):478～502.
邹天人,曹惠志,吴柏青. 1988. 新疆阿尔泰造山花岗岩和非造山花岗岩及其判别标志. 地质学报,62(3):228～243.

The Keke gabbro in Qinghe County of Xinjiang: records from partial melting magma of the oxidized mantle wedge

ZHANG Yong*1), XU Xingwang2)

1) *Tianjin Geological Survey, China Geological Survey, Tianjin*, 300170;

2) *Institute of Geology and Geophysics, CAS, Beijing*, 100029

* *Corresponding author*: *yzhang027@163.com*

Abstract

The Keke gabbro, located in the southeast side at the intersection of Ertix and Koktokay and Ertai faults, South Altay, is one concealed intrusion discovered in recent exploration. In this study, we performed detailed analysis of geological characteristics, geochronology and geochemistry of the Keke gabbro. The results show that the SIMS U-Pb age of zircons from the Keke gabbro is ca 291 Ma, suggesting an age of Early Permian. The Keke gabbro exhibits low SiO_2 (46.14%～52.53%) and MgO (3%～7.68%) contents, with low La/Sm (2.56～4.10) and high $(Gd/Yb)_N$ ratios (1.12～1.61), as well as enrichment of LILE (K, Rb and Pb), and depletion of HFSE (Nb and Ta). Those geochemical characteristics indicate that the magma of the Keke gabbro resulted from partial melting of the oxidized replacement mantle due to subduction, weakly contaminated by crustal materials during its emplacement. Combined with geological and geochemical features, the Permian Keke gabbro in the Altay region formed in extensional tectonic setting, with emplacement of magma controlled by the Ertix strike slipping. Therefore, the gabbro is the important component of the Permian mafic magmatic rocks widely developed in the northern Xinjiang region.

Key words: layered gabbro; geochronology; petrogenesis; Keke district; Altay